Dear Author,

Here are the proofs of your article.

- You can submit your corrections **online**, via **e-mail** or by **fax**.
- For **online** submission please insert your corrections in the online correction form. Always indicate the line number to which the correction refers.
- You can also insert your corrections in the proof PDF and **email** the annotated PDF.
- For fax submission, please ensure that your corrections are clearly legible. Use a fine black pen and write the correction in the margin, not too close to the edge of the page.
- Remember to note the **journal title**, **article number**, and **your name** when sending your response via e-mail or fax.
- **Check** the metadata sheet to make sure that the header information, especially author names and the corresponding affiliations are correctly shown.
- **Check** the questions that may have arisen during copy editing and insert your answers/ corrections.
- **Check** that the text is complete and that all figures, tables and their legends are included. Also check the accuracy of special characters, equations, and electronic supplementary material if applicable. If necessary refer to the *Edited manuscript*.
- The publication of inaccurate data such as dosages and units can have serious consequences. Please take particular care that all such details are correct.
- Please **do not** make changes that involve only matters of style. We have generally introduced forms that follow the journal's style.
  Substantial changes in content, e.g., new results, corrected values, title and authorship are not allowed without the approval of the responsible editor. In such a case, please contact the Editorial Office and return his/her consent together with the proof.
- If we do not receive your corrections **within 48 hours**, we will send you a reminder.
- Your article will be published **Online First** approximately one week after receipt of your corrected proofs. This is the **official first publication** citable with the DOI. **Further changes are, therefore, not possible.**
- The **printed version** will follow in a forthcoming issue.

Please note

After online publication, subscribers (personal/institutional) to this journal will have access to the complete article via the DOI using the URL: http://dx.doi.org/[DOI].
If you would like to know when your article has been published online, take advantage of our free alert service. For registration and further information go to: http://www.link.springer.com.

Due to the electronic nature of the procedure, the manuscript and the original figures will only be returned to you on special request. When you return your corrections, please inform us if you would like to have these documents returned.

Metadata of the article that will be visualized in OnlineFirst

ArticleTitle	Role of the Atlantic Multidecadal Variability in modulating the climate response to a Pinatubo-like volcanic eruption	
Article Sub-Title		
Article CopyRight	Springer-Verlag GmbH Germany (This will be the copyright line in the final PDF)	
Journal Name	Climate Dynamics	

Corresponding Author	Family Name	**Ménégoz**
	Particle	
	Given Name	**Martin**
	Suffix	
	Division	
	Organization	Barcelona Supercomputing Center
	Address	Edifici Nexus II, C/Jordi Girona, 31, 08034, Barcelona, Spain
	Phone	
	Fax	
	Email	martin.menegoz@bsc.es
	URL	
	ORCID	http://orcid.org/0000-0001-7098-9270
Author	Family Name	**Cassou**
	Particle	
	Given Name	**Christophe**
	Suffix	
	Division	CECI
	Organization	Université de Toulouse, CNRS, Cerfacs
	Address	Toulouse, France
	Phone	
	Fax	
	Email	
	URL	
	ORCID	
Author	Family Name	**Swingedouw**
	Particle	
	Given Name	**Didier**
	Suffix	
	Division	
	Organization	UMR CNRS 5805 EPOC-OASU-Université de Bordeaux
	Address	Allée Geoffroy Saint Hilaire, 33615, Pessac, France
	Phone	
	Fax	
	Email	
	URL	

	ORCID	
Author	Family Name	**Ruprich-Robert**
	Particle	
	Given Name	**Yohan**
	Suffix	
	Division	
	Organization	Barcelona Supercomputing Center
	Address	Edifici Nexus II, C/Jordi Girona, 31, 08034, Barcelona, Spain
	Division	CECI
	Organization	Université de Toulouse, CNRS, Cerfacs
	Address	Toulouse, France
	Phone	
	Fax	
	Email	
	URL	
	ORCID	
Author	Family Name	**Bretonnière**
	Particle	
	Given Name	**Pierre-Antoine**
	Suffix	
	Division	
	Organization	Barcelona Supercomputing Center
	Address	Edifici Nexus II, C/Jordi Girona, 31, 08034, Barcelona, Spain
	Phone	
	Fax	
	Email	
	URL	
	ORCID	
Author	Family Name	**Doblas-Reyes**
	Particle	
	Given Name	**Francisco**
	Suffix	
	Division	
	Organization	Barcelona Supercomputing Center
	Address	Edifici Nexus II, C/Jordi Girona, 31, 08034, Barcelona, Spain
	Division	
	Organization	ICREA
	Address	Pg. Lluís Companys 23, 08010, Barcelona, Spain
	Phone	
	Fax	
	Email	
	URL	
	ORCID	

Schedule	Received	16 December 2016

	Revised	
	Accepted	8 October 2017

Abstract	The modulation by the Atlantic multidecadal variability (AMV) of the dynamical climate response to a Pinatubo-like eruption is investigated for the boreal winter season based on a suite of large ensemble experiments using the CNRM-CM5 Coupled Global Circulation Model. The volcanic eruption induces a strong reduction and retraction of the Hadley cell during 2 years following the eruption and independently of the phase of the AMV. The mean extratropical westerly circulation simultaneously weakens throughout the entire atmospheric column, except at polar Northern latitudes where the zonal circulation is slightly strengthened. Yet, there are no significant changes in the modes of variability of the surface atmospheric circulation, such as the North Atlantic Oscillation (NAO), in the first and the second winters after the eruption. Significant modifications over the North Atlantic sector are only found during the third winter. Using clustering techniques, we decompose the atmospheric circulation into weather regimes and provide evidence for inhibition of the occurrence of negative NAO-type of circulation in response to volcanic forcing. This forced signal is amplified in cold AMV conditions and is related to sea ice/atmosphere feedbacks in the Arctic and to tropical-extratropical teleconnections. Finally, we demonstrate that large ensembles of simulations are required to make volcanic fingerprints emerge from climate noise at mid-latitudes. Using small size ensemble could easily lead to misleading conclusions especially those related to the extratropical dynamics, and specifically the NAO.

Keywords (separated by '-')	Volcanic eruptions - Climate dynamics - North Atlantic Oscillation - Atlantic multidecadal variability - Ensemble size - Climate model
Footnote Information	

Role of the Atlantic Multidecadal Variability in modulating the climate response to a Pinatubo-like volcanic eruption

Martin Ménégoz[1] · Christophe Cassou[2] · Didier Swingedouw[3] · Yohan Ruprich-Robert[1,2] · Pierre-Antoine Bretonnière[1] · Francisco Doblas-Reyes[1,4]

Received: 16 December 2016 / Accepted: 8 October 2017

Abstract The modulation by the Atlantic multidecadal variability (AMV) of the dynamical climate response to a Pinatubo-like eruption is investigated for the boreal winter season based on a suite of large ensemble experiments using the CNRM-CM5 Coupled Global Circulation Model. The volcanic eruption induces a strong reduction and retraction of the Hadley cell during 2 years following the eruption and independently of the phase of the AMV. The mean extratropical westerly circulation simultaneously weakens throughout the entire atmospheric column, except at polar Northern latitudes where the zonal circulation is slightly strengthened. Yet, there are no significant changes in the modes of variability of the surface atmospheric circulation, such as the North Atlantic Oscillation (NAO), in the first and the second winters after the eruption. Significant modifications over the North Atlantic sector are only found during the third winter. Using clustering techniques, we decompose the atmospheric circulation into weather regimes and provide evidence for inhibition of the occurrence of negative NAO-type of circulation in response to volcanic forcing. This forced signal is amplified in cold AMV conditions and is related to sea ice/atmosphere feedbacks in the Arctic and to tropical-extratropical teleconnections. Finally, we demonstrate that large ensembles of simulations are required to make volcanic fingerprints emerge from climate noise at mid-latitudes. Using small size ensemble could easily lead to misleading conclusions especially those related to the extratropical dynamics, and specifically the NAO.

Keywords Volcanic eruptions · Climate dynamics · North Atlantic Oscillation · Atlantic multidecadal variability · Ensemble size · Climate model

✉ Martin Ménégoz
martin.menegoz@bsc.es

[1] Barcelona Supercomputing Center, Edifici Nexus II, C/Jordi Girona, 31, 08034 Barcelona, Spain

[2] CECI, Université de Toulouse, CNRS, Cerfacs, Toulouse, France

[3] UMR CNRS 5805 EPOC-OASU-Université de Bordeaux, Allée Geoffroy Saint Hilaire, 33615 Pessac, France

[4] ICREA, Pg. Lluís Companys 23, 08010 Barcelona, Spain

1 Introduction

Large volcanic eruptions impact the climate system through the emission of sulphur compounds that can stay up to several years in the atmosphere if injected into the stratosphere. These compounds are quickly oxidized into aerosols that reduce the downward solar radiation flux leading to tropospheric cooling. Reversely, stratospheric warming occurs through absorption of the upwelling longwave radiation from the troposphere. The eruption of Mount Pinatubo on the Philippine Island Luzon in 1991 is the last big volcanic eruption to date and the associated global cooling at the surface reached about −0.5 °C whereas the stratospheric warming exceeded +1 °C during several months, with regional anomalies exceeding +3 °C (Labitzke and McCormick 1992).

Beyond the lifetime of the volcanic radiative forcing, the persistent dynamical impacts on climate involve the ocean. Recent investigations suggest that large eruptions may drive part of the multi-decadal variability in the Atlantic region through large-scale ocean circulation changes (Stenchikov et al. 2009; Ottera et al. 2010; Zanchettin et al. 2012; Swingedouw et al. 2015). In the Pacific Ocean, proxy-based studies indicate an increase in the probability of occurrence of El Niño episodes during 1–2 years after large tropical

Journal : Large 382	Article No : 3986	Pages : 21	MS Code : CLDY-D-16-00926	Dispatch : 30-10-2017

volcanic eruptions (Adams et al. 2003; Emile-Geay et al. 2008). This response is less clear when assessed from climate models, whose responses to volcanic eruption are ranging from no change in El Niño Southern Oscillation (ENSO) variability (Ding et al. 2014) to very clear evidences for more El Niño events (Hirono 1988; Ohba et al. 2013; Maher et al. 2015). Reconciliation is found in Pausata et al. (2016) and Khodri et al. (2017), showing that the forced-impact on ENSO variability greatly depends on the Pacific Ocean initial state at the onset of the eruption.

At seasonal to intra-seasonal timescales, volcanic eruptions have been shown to affect the North Atlantic Oscillation (NAO, Hurrell et al. 2003) in winter. Over the instrumental period (i.e. from 1850), Christiansen (2008) and Driscoll et al. (2012) observed significant NAO+ phases during the first winter after volcanic eruptions. Based on longer observational datasets, Ortega et al. (2015) used proxy data to reconstruct the NAO index over the last millennium and confirmed the enhanced probability for NAO+ but for the second winter and only for the largest volcanic eruptions (11 eruptions in total, all 10 times stronger than the Pinatubo eruption in terms of ejecta volume). Refining these observational analysis, Swingedouw et al. (2017) also found NAO+ signals, but for the three winters that follow the eight major eruptions of the last millennium, all of them being stronger than Pinatubo. Finally, using climate reconstructions over the last 500 years, Zanchettin et al. (2013a) suggested that the NAO+ signal can persist beyond 3 years and may be even strengthened at decadal timescale through oceanic feedbacks. Collectively, all these studies are indicative of critical limitations in estimating with confidence, from observation only, both timing and robustness of the extratropical responses to volcanic eruptions. Lack of significance is associated with sampling issues with respect to the large internal variability of the NAO. The number of Pinatubo-like eruptions over the instrumental period is very small and the last three biggest volcanic events (Agung, 1963; El Chichón, 1982; Pinatubo, 1991), for which data are the most reliable, are relatively weak compared to the much larger eruptions of the last millennium (Swingedouw et al. 2017). Note also that these three eruptions occurred during strong El Niño events (Robock 2000), which could have blurred any potential volcanically-favored NAO signal.

It thus remains challenging to assess and understand the mechanisms associated with the NAO forced-response to volcanoes. Many studies have highlighted the role of the stratosphere. In his review paper, Robock (2000) evoked the volcanically-enhanced equator-to-pole temperature gradient in the lower tropical stratosphere leading to stronger midlatitude westerly jets through thermal wind relationship. This tends to reinforce the polar vortex favoring *in fine* NAO+ phases through stratosphere-troposphere coupling (Baldwin and Dunkerton 2001). Stenchikov et al. (2002) suggested that the ozone depletion observed after the volcanic eruptions could further contribute to reinforce the polar vortex and related NAO+. This study also highlighted that the volcanically-forced warming in the tropical stratosphere would not impact the polar vortex directly, but rather through changes of tropospheric wave activity. This process has been discussed in Graf et al. (2007) and a more complete picture has been proposed recently by Toohey et al. (2014) and Bittner et al. (2016a). Based on climate models, they showed an equatorward deflation of the tropospheric waves related to the strengthening of the stratospheric zonal circulation at mid-latitudes following the volcanic eruptions. The polar vortex is consequently less disturbed by tropospheric perturbations related to weather noise and is indirectly reinforced. As an additional layer of complexity, the dependence of all these processes to the phase of the Quasi-Biennal Oscillation has been also evoked (Stenchikov et al. 2004; Thomas et al. 2009).

In the historical simulations from the Coupled Model Intercomparison Project (CMIP) archives (Taylor et al. 2012), there is no clear evidence for significant NAO+ signal for the winters following the five largest volcanic eruptions since 1850, neither in CMIP3 (Stenchikov et al. 2006), nor in CMIP5 (Driscoll et al. 2012). Earlier studies (Shindell et al. 2004; Stenchikov et al. 2006) supported the crucial role of stratospheric processes in the modulation of the NAO response to volcanic forcing. These processes are badly reproduced by climate models, even by high-top models where the representation of the stratospheric variability is improved (e.g. Marshall et al. 2009; Charlton-Perez et al. 2013). Toohey et al. (2014) highlighted that the model NAO forced-response could be strongly dependent on the space–time structure of the volcanic aerosol forcing. In addition, very small signal-to-noise ratio may exist for the NAO and, more broadly, for any extratropical dynamical forced response to volcanic eruptions. Accordingly, Bittner et al. (2016b) showed that a minimum of 40 members is necessary to detect a statistically significant strengthening of the polar vortex as a forced response to a Pinatubo-like eruption during the first winter in the MPI-ESM-LR model. Collectively, this succinct review shows that the response of the extratropical dynamics to volcanic forcing is still an open question.

Forecasting the climate response to volcanic eruptions is even more complex in such a context, because of its probable dependence on the mean background climate state and low-frequency climate variability (Zanchettin et al. 2013b). The Atlantic Multidecadal Variability (AMV, Knight et al. 2005; Sutton and Dong 2012; McCarthy et al. 2015) is the main multidecadal phenomenon over a broad North Atlantic/European region; it significantly impacts surface temperature and precipitation over the adjacent continents (Europe, e.g. Sutton and Dong 2012; North America, e.g. Gao et al. 2015;

Journal : Large 382	Article No : 3986	Pages : 21	MS Code : CLDY-D-16-00926	Dispatch : 30-10-2017

the Sahel, e.g. Dieppois et al. 2015). Warm phases of the AMV have been highlighted to favor negative NAO conditions in winter (Sun et al. 2015a; Gastineau and Frankignoul 2015) either through stratospheric or tropospheric pathways (Omrani et al. 2014; Ruprich-Robert et al. 2017, respectively). Yet, despite considerable progress, the drivers of the AMV and associated teleconnections are not fully elucidated and there is a large diversity in the simulation of multi-year AMV-type variability in the CMIP5 models (Martin et al. 2014). Eruptions from El Chichón in 1982 and Pinatubo in 1991 occurred during a cold phase of the AMV, as opposed to Agung eruption in 1963. Noteworthy, the first two winters following Pinatubo and El Chichón last eruptions have been followed by NAO+ whereas NAO− conditions prevailed after Agung eruption (Driscoll et al. 2012). A legitimate question to ask is to what extent the AMV phase has an impact on the overall climate response to the eruptions.

Here, we tackle this key question through a modeling strategy that consists in imposing a fictitious Pinatubo eruption on top of two different AMV-related climate backgrounds extracted from a long control simulation of the CNRM-CM5 coupled model. The details of the experimental setup are given in Sect. 2. Section 3 is devoted to the timing of the atmospheric changes at global scale in response to the volcanic eruption. Section 4 focuses on the impact on the atmospheric circulation over North Atlantic/Europe region and analyses the forced response in terms of weather regimes. Various physical hypotheses to explain the modulation of the changes by the AMV are proposed. Sampling issues are finally discussed. The last section synthesizes the results.

2 Experimental setup

2.1 Model and volcanic forcing

CNRM-CM is the suite of Météo-France ocean–atmosphere coupled model jointly developed by *Centre National de Recherches Météorologiques* (CNRM) and *Centre Européen de Recherche et Formation en Calcul Scientifique* (Cerfacs) research groups. Its third version (CNRM-CM3) produced a significant NAO+ signal for winters following the largest eruptions of the last millennium (Swingedouw et al. 2017). Here we use the fifth version of the model (CNRM-CM5, Voldoire et al. 2013) in low-top configuration. The atmospheric component includes 31 levels with approximately 5 levels from the tropopause to 10 hPa, without any level above the stratopause. The model biases in terms of atmospheric zonal circulation have been drastically reduced in CNRM-CM5 with respect to CNRM-CM3 (see Fig. 5 in Voldoire et al. 2013).

The volcanic forcing comes from Ammann et al. (2007) in both model versions; it is based on the alteration of the zonally averaged aerosol optical thickness (AOT) at a specific stratospheric level and waveband at 550 nm. The Pinatubo forcing used in the following sensitivity experiments is limited to the tropics during the first 6 months following the eruption, with AOT values ranging between 0.2 and 0.3 (Fig. 1). Thereafter, the stratospheric aerosol load progressively increases at middle and high latitudes, with values ranging between 0.1 and 0.2, and concurrently declines in the Tropics. The AOT at high latitudes are greater than in the tropical band from the second winter onwards and it comes back to pre-eruption values after Year 3.

2.2 Sensitivity experiment and protocols

We use the CMIP5 850-year pre-industrial control simulation (piControl) of CNRM-CM5 and select two contrasted AMV periods. Years 141 and 303 (stars in Fig. 2a) are the most extreme years among these periods and serve as initial conditions for the production of two 36-member ensembles of 5-year simulations, hereafter referred to as A-warm and A-cold, respectively. The perturbation for the ensemble generation is limited to the sole atmospheric initial state of the first day integration while the initial conditions for all the other model components are strictly identical. Among 36, 13 members have been extended up to 10 years. Two twin ensemble experiments of same size (therein referred to as PinA-warm and PinA-cold) are conducted with the inclusion of a fictitious eruption of Pinatubo in June of the first year of the integration (see Table 1 for a summary of the simulations).

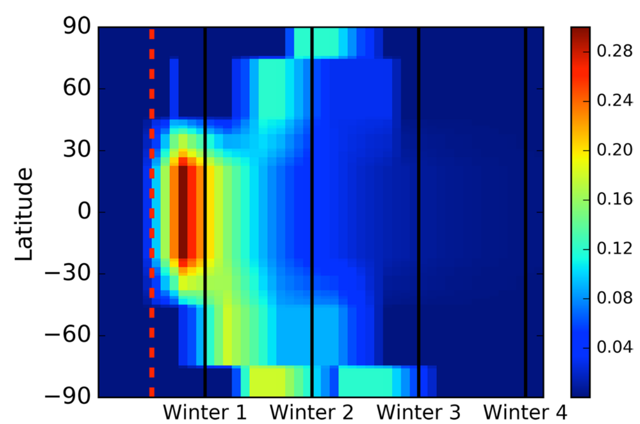

Fig. 1 Latitude-time aerosol optical thickness at 550 nm for the Pinatubo eruption based on the Ammann et al. (2007) reconstruction. The eruption starts in June (red dash line) and vertical black bars position the month of December of the first four winters after the eruption. CNRM-CM5 includes this one wave band volcanic forcing at one stratospheric level

Journal : Large 382 | Article No : 3986 | Pages : 21 | MS Code : CLDY-D-16-00926 | Dispatch : 30-10-2017

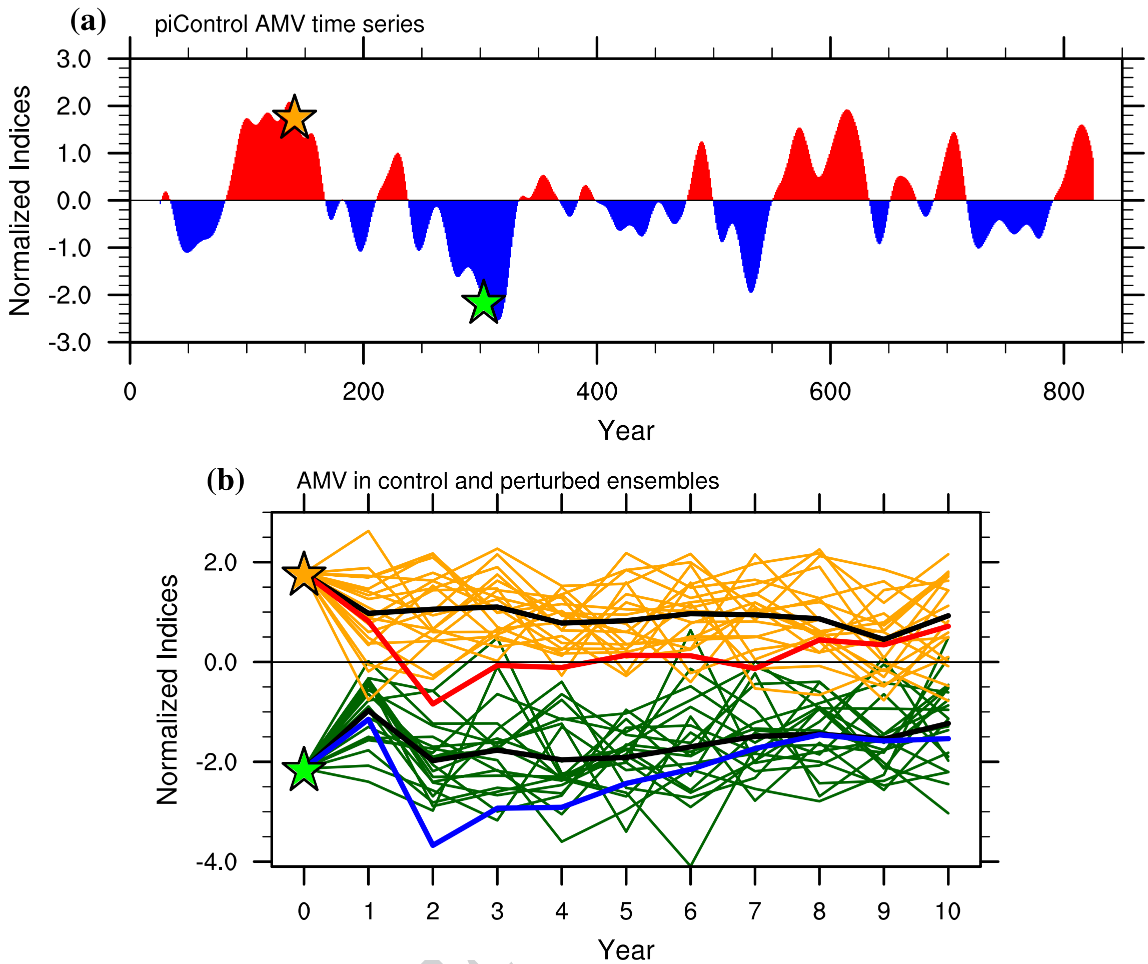

Fig. 2 **a** Annual AMV index defined as the low-pass filtered North-Atlantic SST index using a Lanczos filter (51 weights and a 25-year cutoff period, see Ruprich-Robert and Cassou 2015), computed from the CNRM-CM5 piControl run. The orange and green stars correspond to the years selected for the initialization of A-warm and A-cold ensemble experiments, respectively. **b** Annual AMV index for 13 members of A-warm (orange curves) and A-cold (green curves) ensembles over 10 years. Ensemble means for A-warm and A-cold are in black but in red and blue for PinA-warm and PinA-cold, respectively

Table 1 Summary of the model experiments

Experiment	Initial conditions	External forcing	# Ensemble	Duration (years)
piControl	Model spinup	Pre-industrial	1	850
A-cold	Cold AMV (yr 303)	Pre-industrial	36 (13)	5 (10)
A-warm	Warm AMV (yr 141)	Pre-industrial	36 (13)	5 (10)
PinA-cold	Cold AMV(yr 303)	Pre-industrial + Pinatubo AOT	36 (13)	5 (10)
PinA-warm	Warm AMV(yr 141)	Pre-industrial + Pinatubo AOT	36 (13)	5 (10)

The volcanic forcing induces a decrease of the downward energy fluxes that reaches a maximum of 4 W m^{-2} 6 months after the eruption onset, both at the top of the atmosphere and at the surface (Fig. 3a, b). The global net energy balance of the atmosphere comes back to pre-eruption values around 2 years after the onset of the eruption.

Figure 2b shows a significant initial value predictability of the AMV that persists in both ensembles for at least 10 years. A-cold and A-warm envelops formed by their respective 13 members very rarely overlap and ensemble means are clearly disjoint. In both cases, the Pinatubo eruption leads to surface cooling from Year 2 and its effect persists up to 7-to-9 years; by then the ensemble means of

Journal : Large 382	Article No : 3986	Pages : 21	MS Code : CLDY-D-16-00926	Dispatch : 30-10-2017

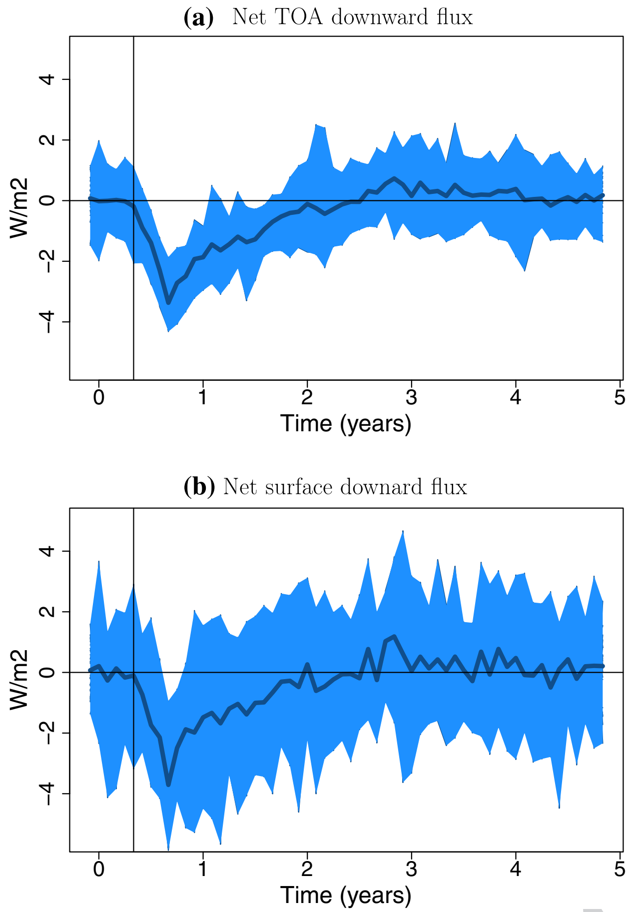

Fig. 3 Energy balance (positive values orientated downward) at the top of the atmosphere (**a**) and the surface (**b**). The 36 member spread (minimum/maximum) appears in light blue and the member mean in dark blue. The Pinatubo eruption is materialized by the vertical bar

perturbed experiments become undistinguishable from their respective control ensembles. In the following we concentrate our study on the first three winters of the ensembles corresponding to the timeslot over which the radiative volcanic forcing goes from maximum to pre-eruption values (Fig. 1).

2.3 AMV fingerprint in CNRM-CM5

Before evaluating the impact of the Pinatubo eruption and its modulation by the AMV phase, multivariate AMV fingerprints of CNRM-CM5 are presented in Fig. 4. Differences between A-cold and A-warm ensembles for surface temperature show a significant cooling over a large part of the Northern Hemisphere; it is particularly pronounced over the mid-to-high North Atlantic and North Pacific Oceans (Fig. 4a). North tropical basins tend to be colder as well whereas positive SST anomalies, albeit weak, prevail in the Southern Hemisphere (south of 20°S). Extreme cooling exceeding − 10 °C from Iceland to Spitsbergen are related to a considerable increase of sea ice concentration in the subarctic Seas and in particular in the Norwegian and the Greenland Seas (Fig. 4b). Our results are consistent with the model interpretations described in Knight et al. (2005). The hemispheric imprint of the AMV in CNRM-CM5 is related to changes in meridional heat transport, especially in the North Atlantic through the alteration of the Atlantic Meridional Overturning Circulation that slackens (increases) before cold (warm) AMV (Ruprich-Robert and Cassou 2015).

Sea level pressure anomalies (SLP) are characterized by a large-scale dipole over a longitudinally extended domain from ~60°W to ~160°E, with positive values over 10°N–70°N and negative values over 10°N–50°S, while wave-train anomalies barely emerge over the Pacific (Fig. 4c). In the North Atlantic sector, SLP changes correspond to a latitudinal tripole between subarctic seas and the Azores; this does not project at all onto the NAO at the surface. Presence of anomalous sea ice in the Nordic Seas (Fig. 4b) is responsible for local positive SLP anomalies that break the basin scale structure of the canonical NAO+ pattern which more clearly emerges in the free atmosphere (Fig. 4d for geopotential at 500 hPa—Z500). Z500 negative anomalies are also significant in the deep tropical band (within 10°N–10°S) in link with overall cold surface conditions there. Using observations and models, Omrani et al. (2014) explained the relationship between cold AMV and NAO+ conditions *via* stratospheric pathways leading to tropospheric changes. We do not expect to reproduce such processes with our low-top model but the AMV imprints in CNRM-CM5 show nevertheless strong similarities with Omrani et al. (2014) patterns in the troposphere.

When zonally averaged, the surface cooling (warming) in the Northern (Southern) Hemisphere extends up to the tropopause, although decreasing with height (Fig. 4e). The meridional temperature gradient is reinforced though the entire atmospheric column in the Northern Hemisphere leading to poleward shift of the mean upper-level westerly jet at mid-latitudes (Fig. 4f). The opposite is found in the Southern Hemisphere with a significant decrease of the mean westerly flow on the equatorward flank of the jet.

3 Global atmospheric forced response to a Pinatubo-like volcanic eruption

3.1 First winter

Figure 5 shows the Pinatubo-forced anomalies for zonally averaged temperature and zonal wind simulated during the first winter (DJFM) after the eruption for cold (a, b)

Journal : Large 382 | Article No : 3986 | Pages : 21 | MS Code : CLDY-D-16-00926 | Dispatch : 30-10-2017

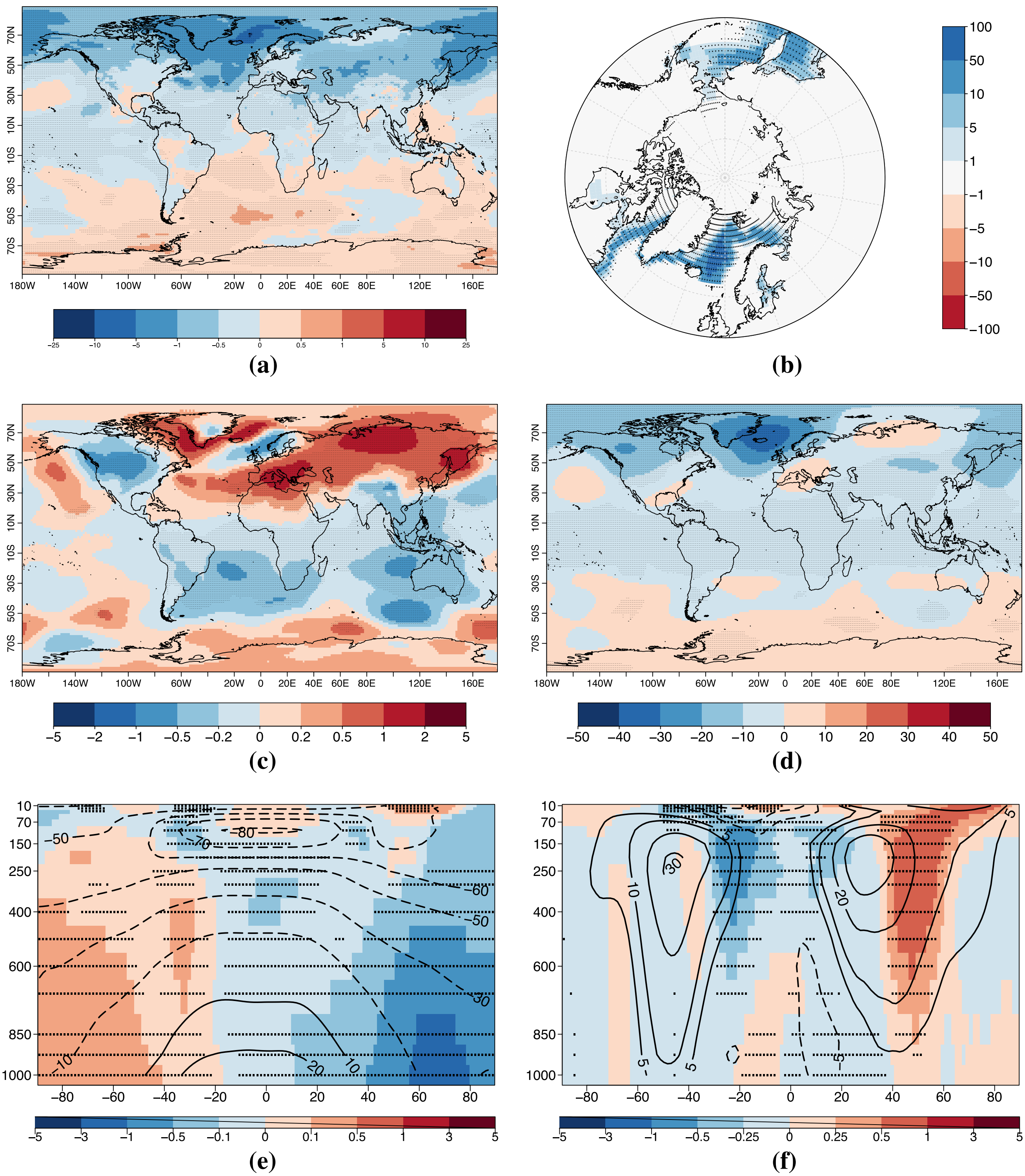

Fig. 4 Differences averaged over the first three winters (DJFM) between A-cold and A-warm ensemble means for surface temperature (**a**), sea ice concentration (**b**), SLP (**c**), geopotential height at 500 hPa (**d**), zonal mean of temperature (**e**) and zonal wind (**f**, eastward positive). Dotted areas stand for significance at the 95% level assessed through bootstrap resampling of the 36-ensemble mean differences. Contours in **e, f** represent the climatology in the A-cold ensemble (solid line for temperature above 0 °C and dashed for those below, solid line for westerly wind counted here positive)

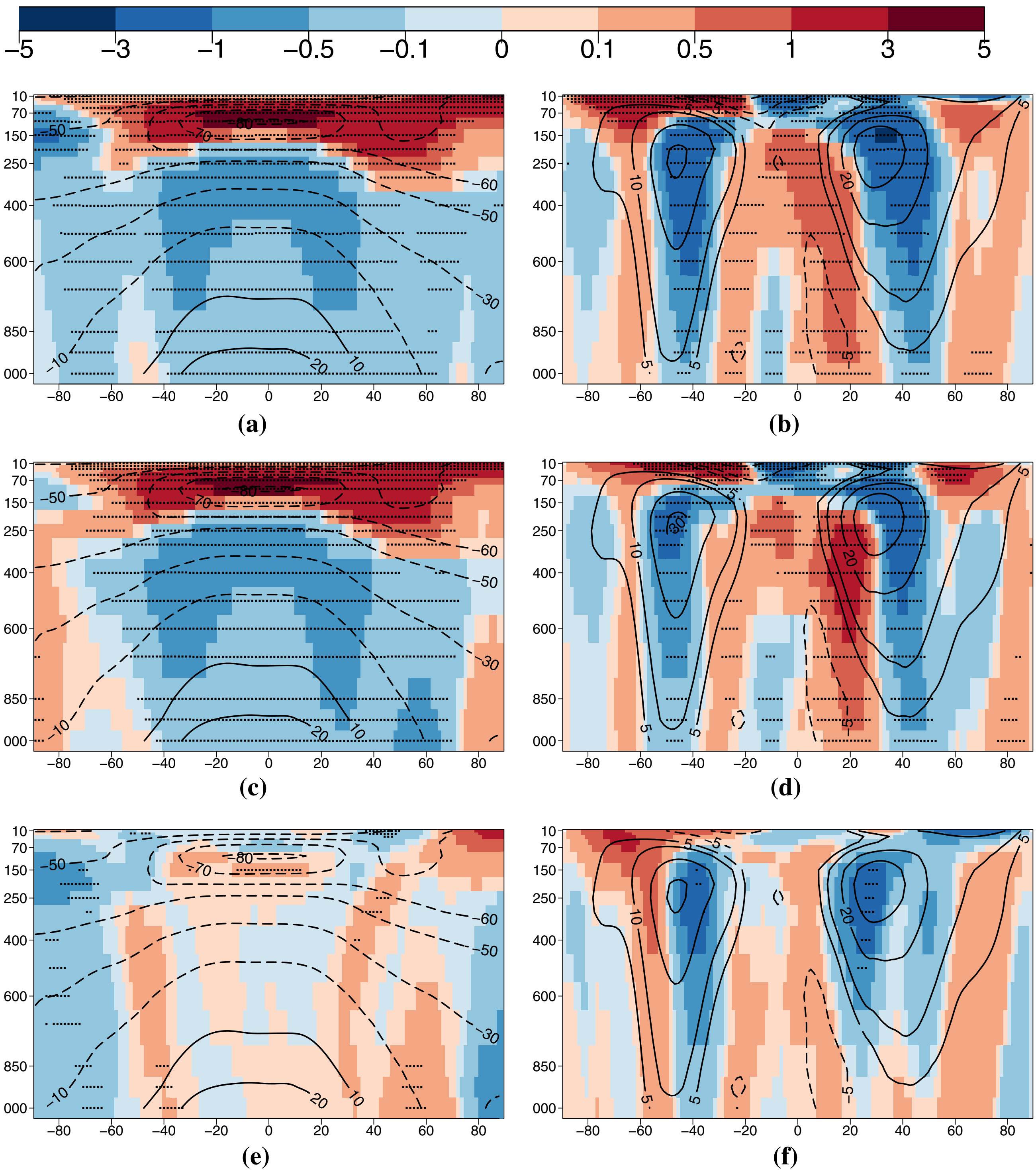

Fig. 5 Difference between PinA-cold and A-cold ensemble means for zonal mean temperature (°C, **a**) and wind (m s^{-1}, **b**, eastward positive) during the first boreal winter (DJFM) after the eruption. **c, d** Same as **a, b** but for PinA-warm—A-warm. **e, f** Show the differences between cold and warm AMV sensitivity experiments (i.e. **e** = **a** − **c** and **f** = **b** − **d**). Dotted areas stand for significance at the 95% level assessed through bootstrap resampling of the 36-ensemble mean differences. Contours represent the climatology for the respective ensemble (solid line for temperature above 0 °C and dashed for those below, solid line for westerly wind counted here positive). The contours shown in **e, f** correspond to the climatology of the A-cold ensemble

and warm (c, d) AMV conditions. The bottom panels (e, f) stand for the differences between the two and should be interpreted as the modulation of the Pinatubo response by the phase of the AMV. The volcanic forcing induces a significant warming of the tropical stratosphere with temperature anomalies locally exceeding 3 °C whatever the AMV phases (Fig. 5a, c). Moderate stratospheric warming also occurs in the Northern latitudes with temperature anomalies of around 1 °C whereas weak stratospheric cooling is found in the high latitudes of the Southern Hemisphere. The high latitude signals in both hemispheres are due to remote dynamical response initiated in lower latitudes, since there is no local forcing related to volcanic aerosols during the first winter (Fig. 1). The Pinatubo eruption induces a general cooling of the troposphere, with values between − 1° and − 0.5 °C in the equatorial and subtropical middle-to-upper troposphere, and between − 0.5° and − 0.1 °C at mid-latitudes in the Northern Hemisphere. These temperature changes are consistent with the observations, both in the stratosphere (Labitzk and McCormick 1992) and in the troposphere (Robock et al. 1995). Differences between the temperature responses with respect to the phase of the AMV are very weak and only limited to latitudes greater than 40° (Fig. 5e). Polar (midlatitude) regions tend to cool more (less) in cold versus warm AMV conditions leading to a meridional temperature anomaly dipole between ~ 50° and ~ 80°. This structure is present in both hemispheres even if maximum significance and vertical extension are found in the southern one.

Consistently with the direct radiative tropospheric cooling that is more pronounced in the Tropics, and the related reduction of the meridional mean temperature gradient, the mean zonal circulation is considerably damped in both AMV cases (Fig. 5b, d). More specifically, a significant decrease is found from the core of the upper-level westerly jets down to the surface in both hemispheres. This contrasts with enhanced values in the equatorial flank of the jets, especially in the Northern Hemisphere; such a latitudinal dipole is suggestive of a contraction of the Hadley circulation. In the stratosphere, the meridional temperature gradient is also reduced, as warming is more pronounced over the cold climatological core in the tropical low stratosphere (Fig. 5a, c). This leads to a weakening of the thermally-driven jets at mid-latitudes in the Northern Hemisphere. A moderate acceleration of the westerly circulation is found between 10 and 100 hPa in the northern hemisphere high latitudes (Fig. 5b, d, ~ 1 m s^{-1}), consistently with the local increase of the temperature meridional gradient at ~ 70 hPa between 60°N and 90°N (Fig. 5a, c); this is indicative of a reinforcement of the polar vortex. We recall here that caution should be used when interpreting stratospheric signals because of the coarse vertical resolution above the tropopause in the low-top version of CNRM-CM5. Differences between the zonal wind responses to a Pinatubo eruption in cold versus warm AMV ensembles are marginal (Fig. 5f). The only significant impact of the AMV is found in the upper-troposphere, where the equatorial flank of the jets is more reduced in case of cold versus warm AMV conditions, a difference more pronounced in the Northern Hemisphere.

Weakening of the mid-latitude jet streams on their polar flank and concurrent equatorward shift correspond to a mean circulation that is not favourable to NAO+ conditions (Tanaka and Tokinaga 2002; Scaife et al. 2005). Nevertheless, a change of zonal circulation in the polar stratosphere is not a sufficient condition to affect the NAO at the surface (Bittner et al. 2016b). Downward stratospheric forcing can be too weak to be detectable in presence of very large internal variability (Bittner et al. 2016b) or too confined in the high latitudes (north of 60°N) to affect the intrinsic modes of the large-scale North Atlantic atmospheric variability, as suggested in Barnes et al. (2016), Zambri and Robock (2016) and found in our case with CNRM-CM5.

3.2 Third winter

In the following, we directly jump to the description of the third winter since the zonal response in Year 2 is very similar to Year 1, albeit weakened (not shown). In DJFM of Year 3, there is no direct radiative forcing from volcanic particles in the Northern Hemisphere (Fig. 1), and only indirect effects associated with atmosphere/surface coupling can explain the volcanic-forced response depicted below. The stratospheric warming disappears but the tropospheric cooling remains strong and statistically significant in the order of − 0.5 °C in both AMV conditions (Fig. 6a, c). This is particularly true in the Tropics and the temperature meridional gradient is still reduced in the upper troposphere inducing a strong weakening of the equatorward flank of the jets (− 1 to − 3 m s^{-1}) in both hemispheres (Fig. 6b, d). Closer to the surface, cooling of about − 1 °C occurs at polar latitudes in the Northern Hemisphere (north of 60°N, below ~ 700 hPa) leading to increased low-level meridional gradient between mid and high latitudes (Fig. 6a, c) and enhanced zonal circulation, albeit not significant, between 40°N and 60°N on the polar side of the jet (Fig. 6bd). The sole AMV-attributable modulation of the volcanic-forced response is found for the westerly circulation between 20° and 40° of latitude in both hemispheres (Fig. 6f). When the AMV is cold, the weakening of the subtropical jets is much more pronounced and extends down to the surface (Fig. 6b), whereas it is rather confined to the deep Tropics and upper-level troposphere/low stratosphere in the warm phase of the AMV (Fig. 6d).

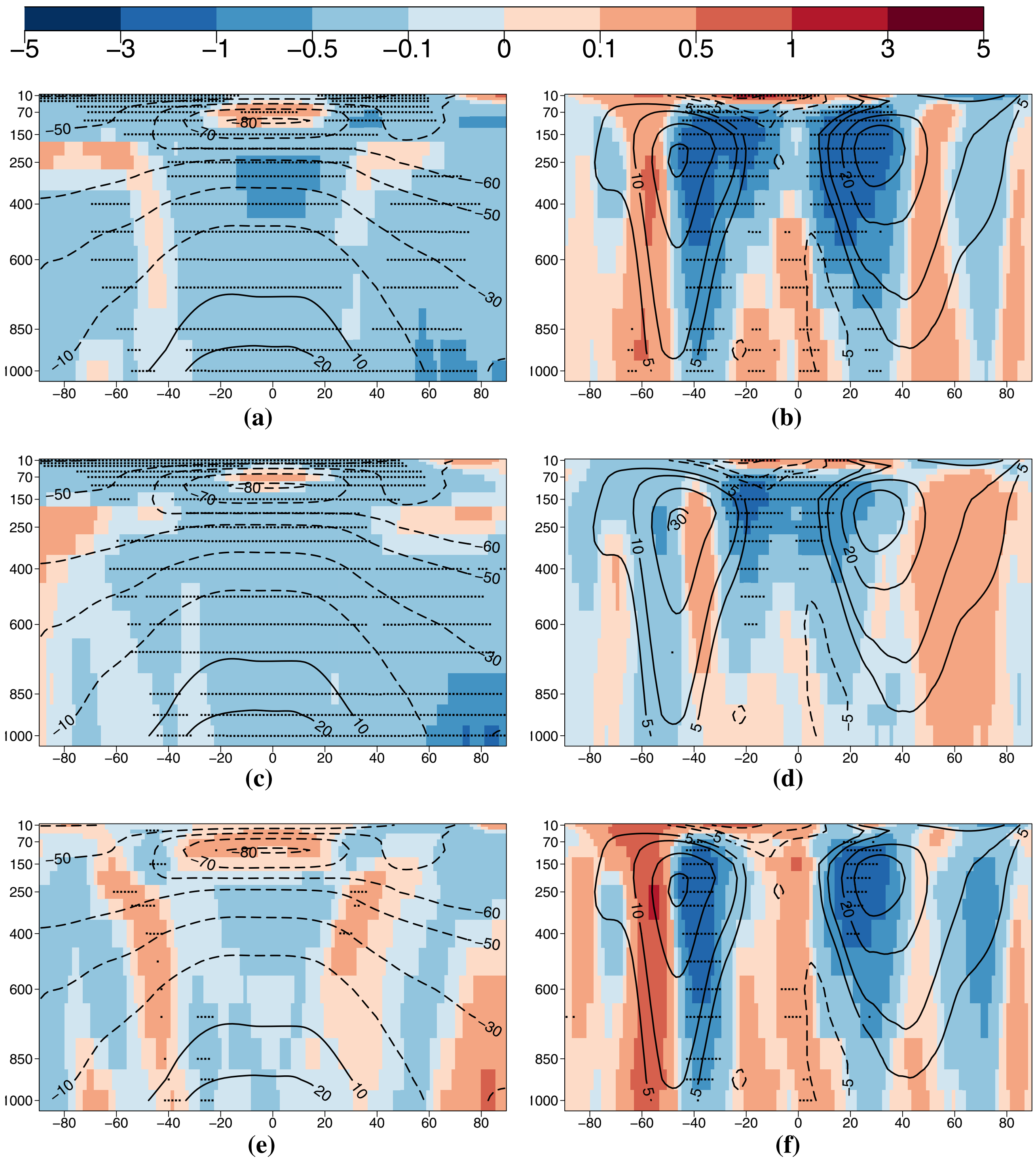

Fig. 6 Same as Fig. 5, but for the third boreal winter after the volcanic eruption

Zonal means, which are relevant to assess changes in global equilibria, can hide more pronounced basin-scale signals due to local feedbacks and/or particular geometry of the climatological dynamics. The sensitivity of the volcanic-forced response to the phase of the AMV is now investigated regionally over the North Atlantic sector.

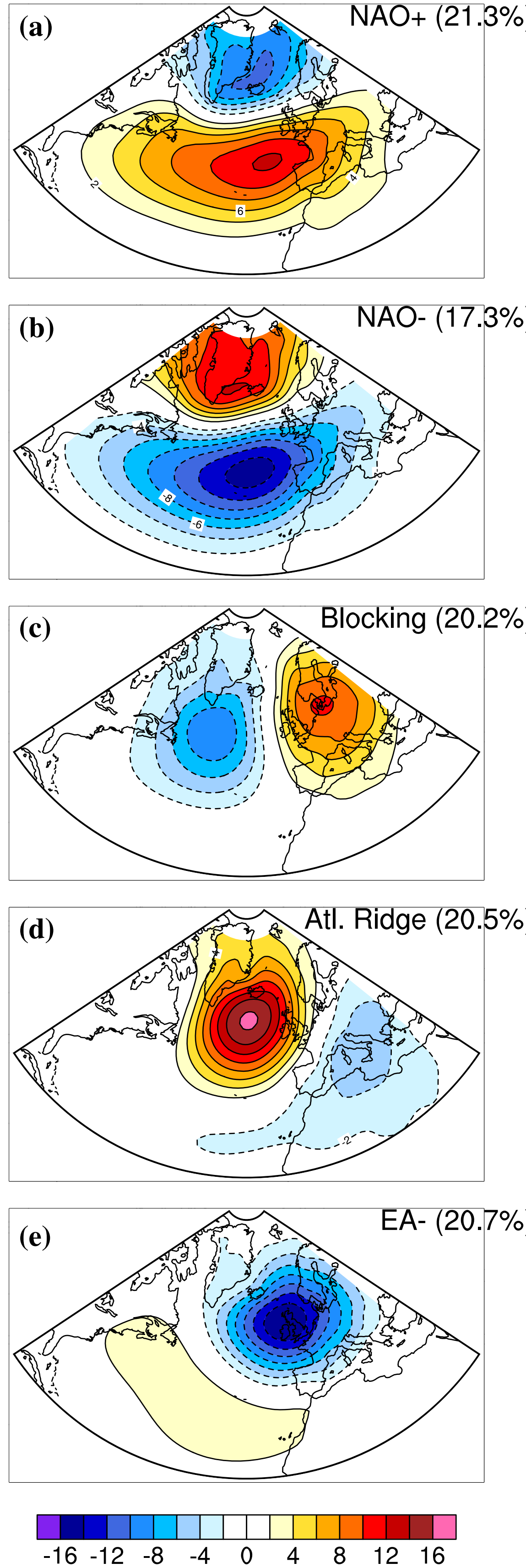

Fig. 7 Centroids of the five wintertime North Atlantic weather regimes obtained from daily anomalous mean sea level pressure maps from piControl. Each percentage corresponds to the mean occurrence of the regime computed over 850 years. Contour interval is 2 hPa

4 Wintertime North Atlantic atmospheric forced response to a Pinatubo-like eruption

4.1 Weather regimes

The modulation of the Pinatubo-forced atmospheric response by the AMV is assessed over the North Atlantic sector through the weather regime paradigm (Vautard 1990). Based on clustering techniques, weather regimes (WRs) can be viewed as the preferential states of the atmospheric circulation on a daily basis and the day-to-day meteorological fluctuations can be interpreted in terms of temporal transitions between regimes. We use wintertime daily sea-level pressure maps from the 850-yr piControl experiment and perform a regime decomposition based on the *k-means* algorithm. The most robust partition following Michelangeli et al. (1995) criteria to evaluate the significance of the decomposition, is obtained for $k = 5$ in CNRM-CM5 as opposed to $k = 4$ in the observations (the reader is invited to refer to Cassou 2008 for a complete description of the regime determination). The positive and negative NAO regimes, also referred to as Zonal and Greenland Anticyclone circulations respectively, are relatively well-represented in the model, although too spatially symmetrical compared to observations (Fig. 7a, b). The Blocking (BL) and Atlantic ridge (AR) regimes are also relatively well-captured (Fig. 7c, d). The fifth weather regime is characterized by negative SLP anomalies over the UK (Fig. 7e). It projects upon the negative phase of the East Atlantic Pattern and will be termed accordingly by EA−. The presence of EA− is associated with climatological biases in CNRM-CM5, which tends to simulate too zonal and eastward-displaced storm-track/upper-level jet off Western Europe (see Voldoire et al. 2013, their Fig.3). The Pinatubo-forced signal and its modulation by the AMV are investigated here on an interannual basis through changes in the distribution of the WR occurrences computed separately for each member and each ensemble. Technically, daily anomalous sea level pressure maps for the winter season only (1st Dec. to 31st Mar.) are first projected onto the 5 WR centroids and then attributed to the closest one based on Euclidian distances. This operation is repeated for the 36 members and statistics are built per winter for the A-cold and A-warm ensembles and their respective PinA-cold and PinA-warm perturbed ones, all taken individually.

The volcanic forcing does not induce any significant change in WRs occurrences in Winter 1 and Winter 2 as further commented in Sect. 4.4. Significant alteration is only found during the third winter and only for cold AMV

Journal : Large 382	Article No : 3986	Pages : 21	MS Code : CLDY-D-16-00926	Dispatch : 30-10-2017

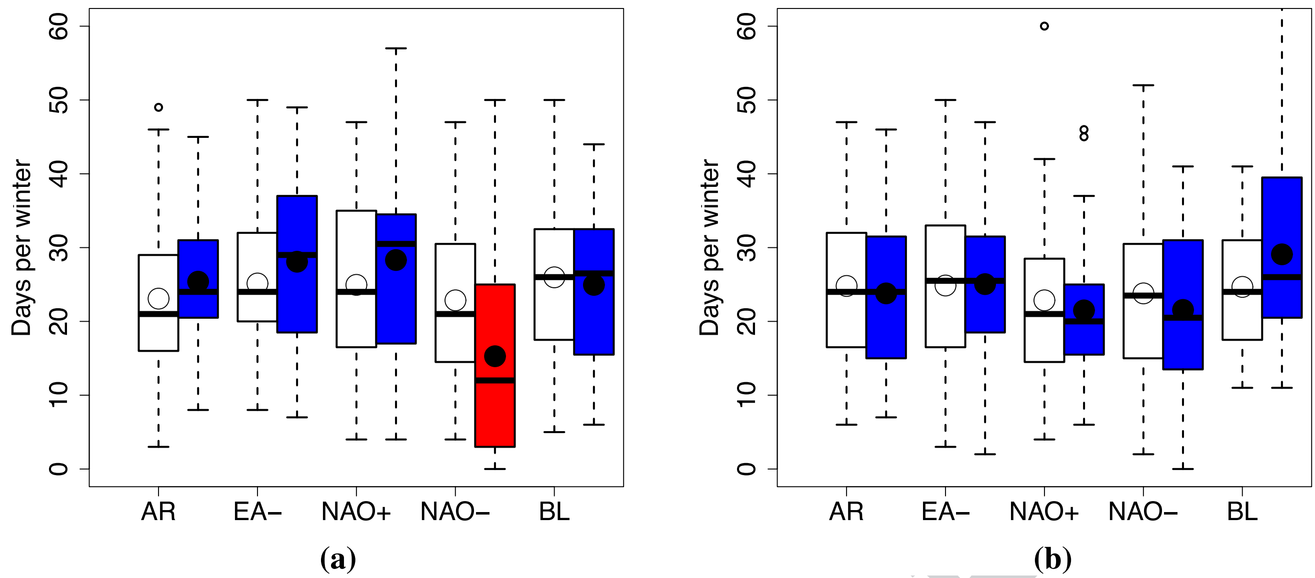

Fig. 8 Number of day statistics of each of the five weather regimes and for each ensemble for cold (**a**) and warm (**b**) AMV conditions. Results for A-cold and A-warm are in white while PinA-cold and PinA-warm are in red when the difference between their respective control simulations is significant at the 99% confidence level assessed through bootstrap resampling, blue otherwise. Large circles and horizontal bolt lines stand for the mean and median of the WR distribution. The box plots show the first and the third quartiles (Q1 and Q3), the whiskers the quantiles $Q1–1.5\times(Q3-Q1)$ and $Q3+1.5\times(Q3-Q1)$, whereas small circles are considered as outliers of the distribution

conditions (Fig. 8). There is a drastic decrease in the occurrence of the NAO− regime dropping from 23 to 15 days ($\sim -35\%$) on average over the 36 members. This reduction is compensated by a slight increase of occurrence of the four other regimes. This NAO− signal is highly significant (p-value = 0.006) whereas the modifications for the others are not (p-values higher than 0.1). In warm AMV conditions, the average number of NAO− days is marginally affected by the volcanic forcing, going from 24 to 22 days on average (p-value = 0.19), but none of the WRs change is detectable (signals smaller than 2 days and p-values greater than ~0.2). It is interesting to stress out here that changes in NAO− WR statistics are not compensated by any significant modification of NAO+. This is suggestive of an asymmetrical response of the NAO to the volcanic forcing. We computed a traditional NAO index based on Empirical Orthogonal Functions (EOF) and found positive values in Winter 3 but only significant at the 80% level of confidence (not shown). This confirms the added value of regime approaches versus linear techniques assuming symmetry and orthogonality of the modes of variability. We got similar findings when projecting modeled outputs onto observed WR centroids instead of modeled ones (not shown). This suggests that the NAO signal detected is not depending on the model NAO centroid biases. The physical causes of the NAO− decrease in Winter 3 during cold AMV in response to the volcanic forcing is now investigated.

4.2 Tropical teleconnection

When the AMV is cold, the deficit of NAO− WR during the third winter after a Pinatubo-like eruption is in fact the regional signature of a broader large-scale modification of the atmospheric circulation (Fig. 9a). Subtropical highs are reinforced in both the North Pacific and the North Atlantic and form a connecting V-shape pattern. At high latitudes, Aleutian and Icelandic Lows are more pronounced. In the Tropics, a seesaw pattern is found between the Eastern and Western Pacific basins, with some extension over the Indian AQ4 Ocean. This is typical for La Niña teleconnections in relation with enhanced Walker cell circulation (Bjerknes 1969; Trenberth et al. 1998) as confirmed in Fig. 9b, which shows the 2-m temperature (SAT) forced-response for the cold AMV conditions. Strong cooling is found along a wide Pacific cold tongue but also in the other tropical basins to a lesser extent. This is consistent with the negative temperature anomalies over the entire troposphere during the third winter after the eruption as detailed earlier in Sect. 3.2 (Fig. 6a). AQ5 In the Southern Hemisphere, zonal anomalies project onto the positive phase of the Southern Annular Mode (SAM) in coherence with La Niña forcing (Cai and Rensch 2013).

The direct forcing of the volcanic aerosols become negligible in Year 3 (Fig. 1) and therefore the tropospheric and surface cooling in the Tropics should be interpreted at this time as the result of the ocean memory of the radiative deficit of the previous 2 years and notably as a dynamical effect

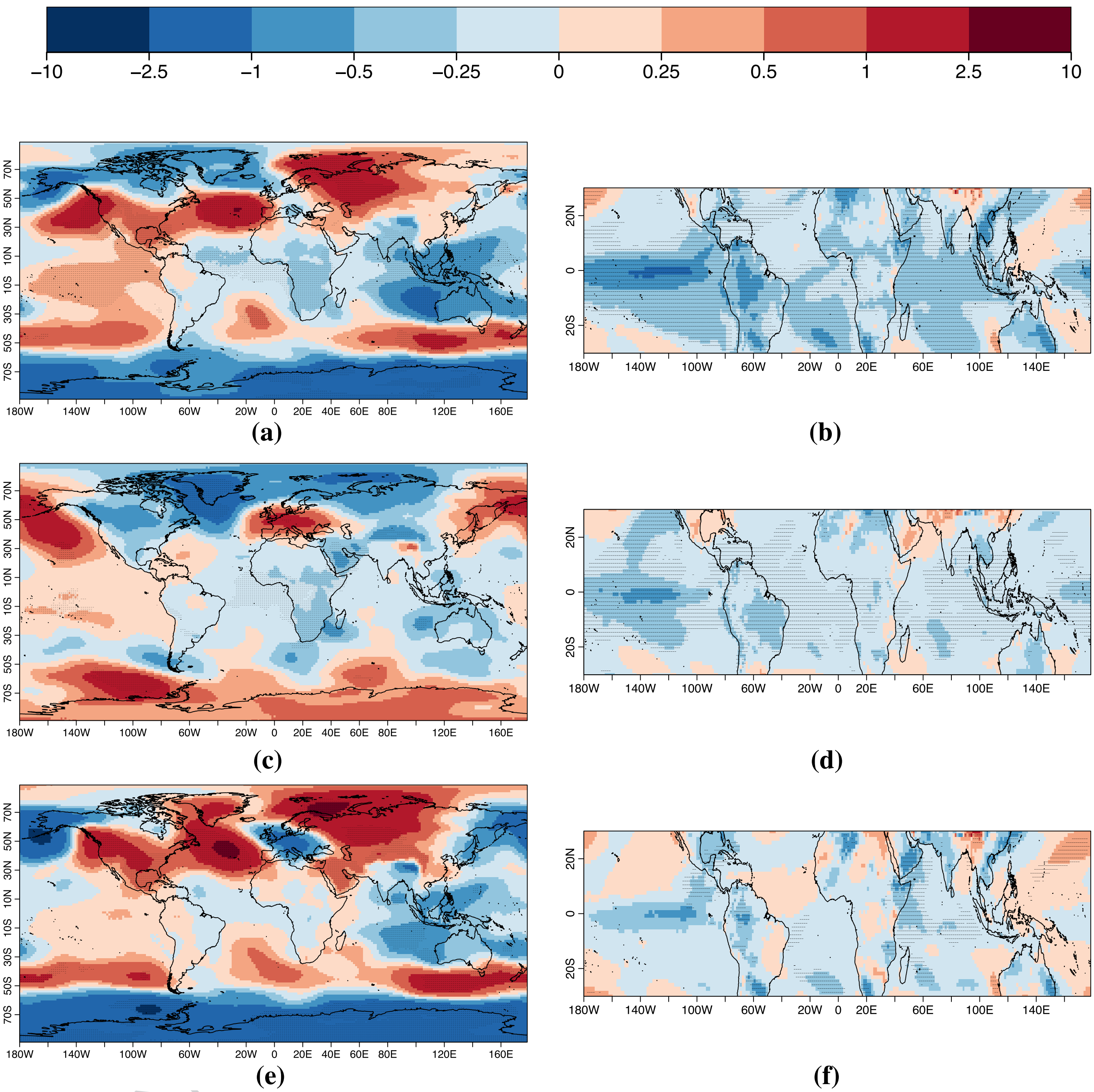

Fig. 9 Same as Fig. 6 but for Sea Level pressure anomalies (**a, c, e**) and 2-m temperature anomalies (**b, d, f**) modeled the third boreal winter after the volcanic eruption

due to La Niña as we shall describe in the following. The ENSO response to volcanic forcing is complex but there is an emerging consensus that El Niño events are favored during the first and even more likely the second year after the volcanic eruption (e.g. Swingedouw et al. 2017; Khodri et al. 2017). According to Maher et al. (2015), such a dynamical response of ENSO can be explained through the dampening of the trade winds, consistent with the contraction of the Hadley cell, which we accordingly simulated in our model (Fig. 6). Figure 10 shows the relative SST anomalies (SSTA) over the Niño 3.4 region that is defined in Khodri et al. (2017) as the difference between SSTA over the Niño 3.4 region and the SSTA averaged over the entire tropical band (20°S–20°N). This allows an assessment of ENSO in presence of overall cooling due to radiative volcanic-forced effect. The A-cold experiment has been initialized during an El Niño event and produces a La Niña episode in Year 1, then followed by weak warm ENSO events on average in

Journal : **Large 382** | Article No : **3986** | Pages : **21** | MS Code : **CLDY-D-16-00926** | Dispatch : **30-10-2017**

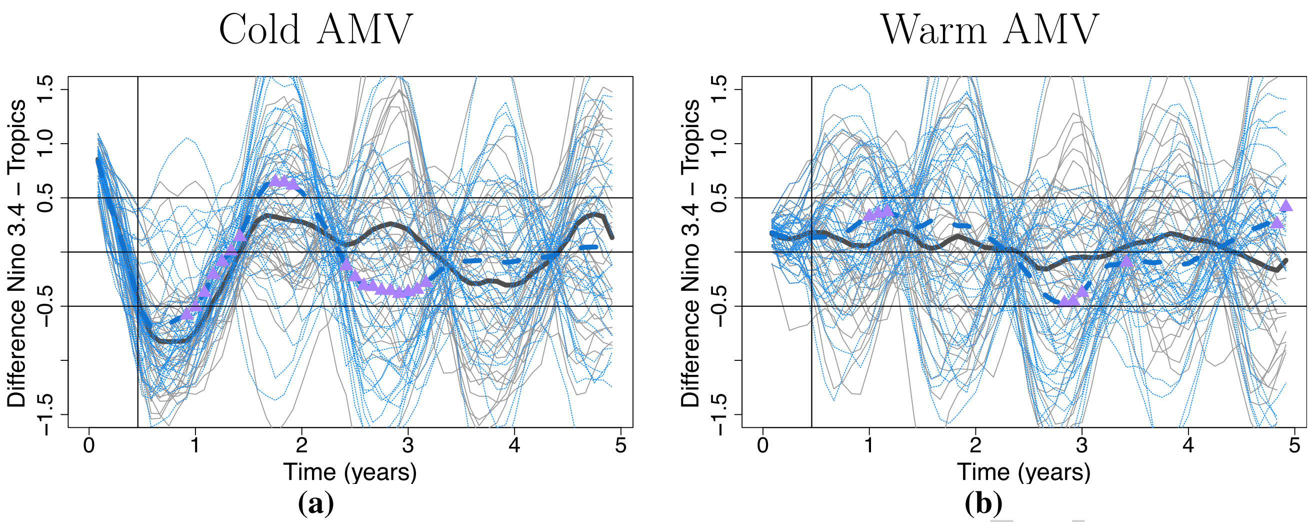

Fig. 10 SSTA index simulated under cold (**a**) and warm (**b**) AMV conditions. Following Khodri et al. (2017), the SSTA index is defined as the relative SST anomaly over the Niño 3.4 region (5°S–5°N; 170°W–120°W) with respect to the SST anomaly over the tropical ocean belt (20°S–20°N). The time series are filtered out with a 3-month running mean. In the Niño 3.4 region, El Niño (la Niña) events are defined when the temperature anomaly exceeds (−) 0.5 °C during more than 3 consecutive months. Purple triangles pointed down appear for the significance assessed trough bootstrap resampling of the 36-ensemble mean differences between the control (black line) and the Pinatubo (blue line) experiments

Year 2 and 3, albeit not significant. The Pinatubo eruption diminishes a bit the strength of the La Niña event in Year 1, but considerably reinforces the following warm ENSO episode in Year 2. El Niño events are likely to be followed by La Niña conditions (e.g. Bjerknes 1966, 1969; Cane and Zebiak 1985; Dinezio et al. 2017) and this pendular behavior is exacerbated here for Year 3 in the PinA-cold ensembles.

When the AMV is warm, the changes in circulation in Winter 3 are considerably smaller. Although present, the La Niña response is less pronounced and the associated teleconnections are almost inexistent in both the tropics and the mid-latitudes whatever the hemisphere (Fig. 9c, d). A-Warm ensembles have been initialized in ENSO neutral phase (Fig. 10b). Accordingly, there is no alternation between La Niña and El Niño events in Year 1 and Year 2, respectively. Yet, it is noteworthy that La Niña conditions prevail in Year 3 in PinA-warm like in PinA-cold.

The difference between the two responses with respect to the phase of the AMV is given in Fig. 9e, f for SLP and SAT, respectively. In the Northern Hemisphere, it is dominated by a wave train pattern that originates in the Caribbean and ends around the Arabic peninsula; this wave train almost extends along a great circle with maximum cores of opposite signs over the Azores and Europe. This structure is reminiscent of a forced Rossby wave arising from the western tropical Atlantic/Eastern Pacific Warm Pool (EPWP) region in link to local colder anomalies, as shown in Fig. 9f. It is consistent with Terray and Cassou (2002, their Fig. 10) findings and also Cassou et al. (2004, their Fig. 8) who provided evidence that cold conditions over a broad tropical western Atlantic sector diminish local diabatic heating and inhibit *in fine* the excitation of NAO− regimes. In addition, overall enhanced sensitivity to volcanic forcing in the cold AMV ensemble can be associated with the change in the mean climate background state as illustrated in Fig. 4 and in particular to the modification of the mean meridional temperature gradient as well as the general tropical cooling that affects the convection and the strength of the Walker cell (Bony et al. 2015). SAT anomalies are much more negative in cold AMV phase and leads to stronger teleconnection originating from the Indo-Pacific region, especially in the Southern Hemisphere.

Finally, it is interesting to note that significant high pressure anomalies are found in the cold AMV case in the Barents Sea and western Siberia as well as in the Labrador Sea (Fig. 9a). This is precisely the region where mean sea ice cover greatly differs between the two phases of the AMV. The sensitivity of the Pinatubo-forced response to sea ice conditions is investigated below.

4.3 Sea ice anomalies

Change in sea ice concentration is a potential driver for the alteration of the wintertime circulation at mid-latitudes. Several studies (Peings and Magnusdottir 2014; Harvey et al. 2014, 2015; Sun et al. 2015b; Deser et al. 2016) suggested that reduced sea ice cover in the Arctic would induce a slackening of the mean zonal circulation, with an eventual lag of 1–3 months and would favor NAO− conditions over the North Atlantic (Oudar et al. 2017). In our experiments, sea ice increases in the Arctic in response to the Pinatubo

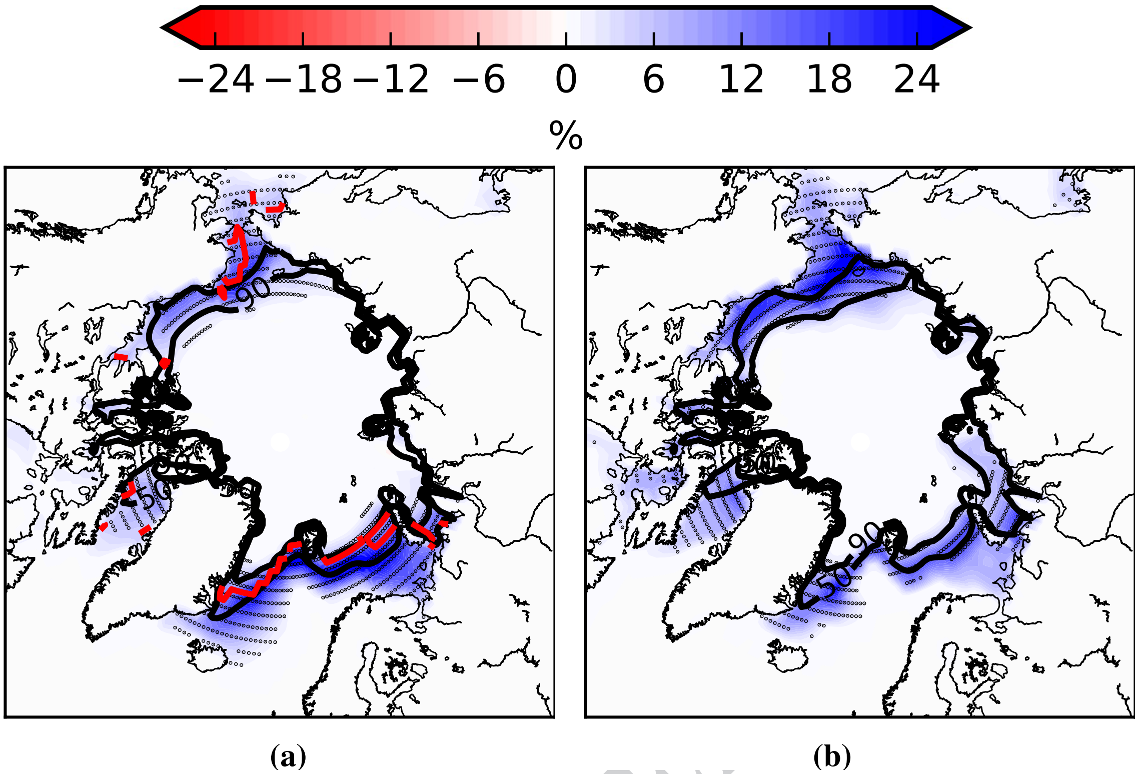

Fig. 11 Difference between PinA-cold and A-cold (**a**) and PinA-warm and A-warm (**b**) ensemble means for sea ice concentration anomalies (shading, %) during the third autumn (October–November) following a Pinatubo eruption. Dotted areas stand for significance at the 95% level assessed through bootstrap resampling of the 36-ensemble mean differences. Contours stand for climatological 50% and 90% levels for the A-cold (**a**) and A-warm ensemble (**b**). Areas located south of the red contours in (**a**) show the regions where the increase of sea ice is stronger in cold versus warm AMV conditions

eruption and reaches its maximum value in Year 3 independently of the phase of the AMV (not shown). In autumn of that year, sea ice dramatically grows southward from the Arctic, with anomalies varying between + 10 and + 25% in the Northern Pacific and in the Northern Atlantic subarctic basins (Fig. 11a, b). This signal, persisting from the autumn to the winter, clearly explains the tropospheric cooling simulated in the Northern high latitudes (Fig. 6a, c). The southward extension of the sea-ice is more pronounced in cold versus warm AMV conditions (Fig. 11a, red line), inducing a stronger cooling between 40°N and 60°N in the case of the cold AMV situation with respect to the warm AMV situation (Fig. 6e). On the contrary, the cooling modeled between 60°N and 90°N is more pronounced in the case of the warm situation (Fig. 6e). These differences of zonal mean temperature have to be considered carefully since they are not significant and may not describe correctly the regional impacts of Arctic sea-ice.

To gain insight into the potential role of the Arctic in the greater inhibition of the NAO− regimes in cold AMV conditions in response to volcanic forcing, we investigate the model NAO intrinsic sensitivity to the variability in Arctic sea ice extent (SIE) from the 850-year control simulation. SIE values are binned in quantiles and the corresponding mean occurrences for NAO− regimes are computed. Because we want to evaluate the forcing role of SIE onto North Atlantic atmospheric dynamics, a 2-month lag is introduced and Fig. 12 presents the relationship between October–November (ON) SIE and the following wintertime NAO− regimes for piControl (grey dots) and the four ensembles (stars) for the third winter after the eruption. From this figure, we can see that, in CNRM-CM5, autumn SIE in the Arctic can be interpreted as one of the predictors for NAO− occurrence (about ~ 20% of explained variance). Despite considerable spread, positive SIE anomalies tend to inhibit the next wintertime excitation of NAO− (lower right quadrant) in line with the conclusions of Oudar et al. (2017). In our Pinatubo sensitivity experiments, cooling leads to SIE increase in the Arctic, which indirectly disfavors NAO− occurrence in both AMV phases. However, it is interesting to stress out that autumn SIE in the PinA-cold ensemble corresponds to record high values (blue stars) that are not "compatible" with internal variability assessed in piControl. We suspect that these extreme SIE conditions in the Arctic could partly explain the large deficit of NAO− days in PinA-cold. The fact that

Journal : Large 382	Article No : 3986	Pages : 21	MS Code : CLDY-D-16-00926	Dispatch : 30-10-2017

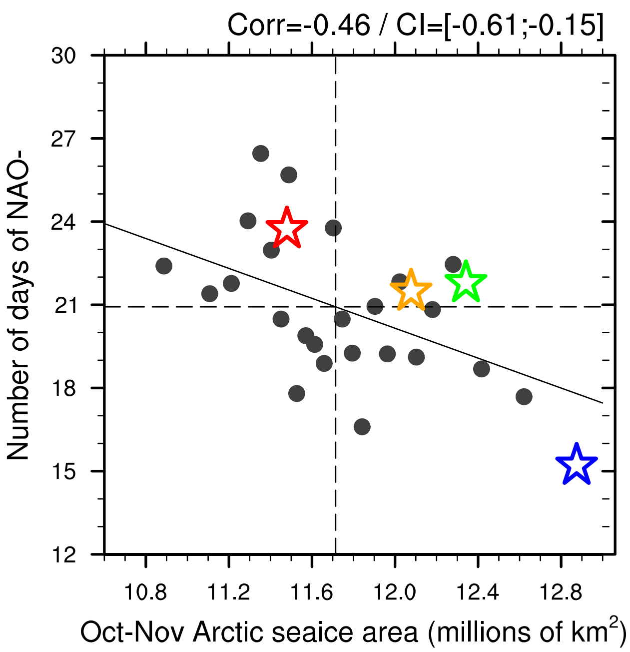

Fig. 12 Relationship between Winter NAO− occurrence and Arctic autumn SIE. SIE from piControl are binned into 24 quantiles (grey dots) to include a number of samples that is comparable with the size of the ensemble experiments (36 members) whose ensemble means are represented by the stars (green for A-cold, blue for PinA-cold, *red* for A-warm and orange for PinA-warm). The average number of NAO− per quantile is given by the grey dots. A simple regression line is added and the correlation r is shown in the right upper-side of each panel. The 5% and 95% lower and upper confidence bounds for r are given in brackets based on the generation of 5000 bootstrap data samples following (Mudelsee 2014). When the confidence interval excludes 0, the null hypothesis r = 0 is rejected at a 95% level

the decrease of the NAO− occurrence is more pronounced in cold versus warm AMV experiments would rely on polar amplification mechanisms acting when extreme values of SIE are present, and in particular in a "never-happened" situation such as produced in PinA-cold. This non-linear hypothesis is impossible to be confirmed from solely control experiments and would require dedicated sensitivity ensemble.

4.4 Statistical significance and sampling issues

We have shown that the signal-to-noise ratio related to the volcanic forcing on the extratropical circulation is low in the model (Fig. 6). The statistical robustness of changes in NAO WR occurrence is now evaluated as a function of the ensemble size for the first and third winters (Figs. 13, 14, respectively). To do so, a bootstrap resampling (200 times with replacement) of the members is applied and the envelope built from the grey curves represents the possible outcomes for the difference of NAO WR occurrence between PinA-cold (eventually PinA-warm) and A-cold (eventually A-warm) as a function of the size of the ensembles (left panels). The green curve stands for the mean of the grey curves and the blue curve represents the actual changes going incrementally from 2 to 36 members. By construction, blue and green curves eventually converge. To draw firm conclusions about the significance of the WR changes, the p-value of the difference is provided as well as an objective evaluation of the power of the test that has been used to compute this p-value (right panels), here based on bootstrap resampling (10,000 times with replacement) of N members available (x-axis). The blue curve provides the p-value computed by using members going incrementally from 2 to 36. The grey curves show p-values computed with samples of N members from a bootstrap resampling (200 times with replacements) of the whole set of 36 members, on which we apply the above-described statistical test. The power of the test is defined as the probability that the test gives a p-value below the 0.05 threshold (level chosen classically for significance). Siegert et al. (2017) point out that a power of the test higher than 80% should be required to prove that a result is effectively significant in climate forecast verification, as it is commonly admitted in medical sciences.

Based on 36 members, we provide evidence that there is no NAO response in CNRM-CM5 during the first winter after the volcanic eruption (Fig. 13). Interestingly, misleading and non-robust conclusions could have been drawn if the ensemble size had been between 6 and 10 members. The blue curve for NAO− then shows enhanced occurrence by around 10 days (Fig. 13a) that is partly compensated with NAO+ deficit (Fig. 13b) for such a size of the ensembles. We could even have had some confidence in the significance of the NAO− WR changes since the corresponding p-value was close to 0.05. Nevertheless, the power of the test never exceeds 10% and does not increase with the ensemble size, both for NAO+ and NAO− WRs. Therefore, based on CNRM-CM5, we conclude that first year NAO signals can be obtained by pure chance if the ensemble size is too small and the significance not thoroughly tested.

As documented above, the strongest signal that we obtained in response to volcanic eruption is for NAO− during the third winter. Figure 14a, b confirms that the NAO− deficit in AMV cold conditions is very robust with a p-value reaching 0.006 and a power of the test that constantly increases with the ensemble size and reaches 80% with 36 members. In the warm AMV conditions, the NAO− deficit is smaller and less significant with a p-value equal to 0.19 with 36 members and a power that barely reaches ~ 20% (Fig. 14c, d). Note though that the p-values are decreasing and the power is slightly increasing with the number of members so that we may eventually expect this NAO− signal to become significant for a larger ensemble

Journal : **Large 382** | Article No : **3986** | Pages : **21** | MS Code : **CLDY-D-16-00926** | Dispatch : **30-10-2017**

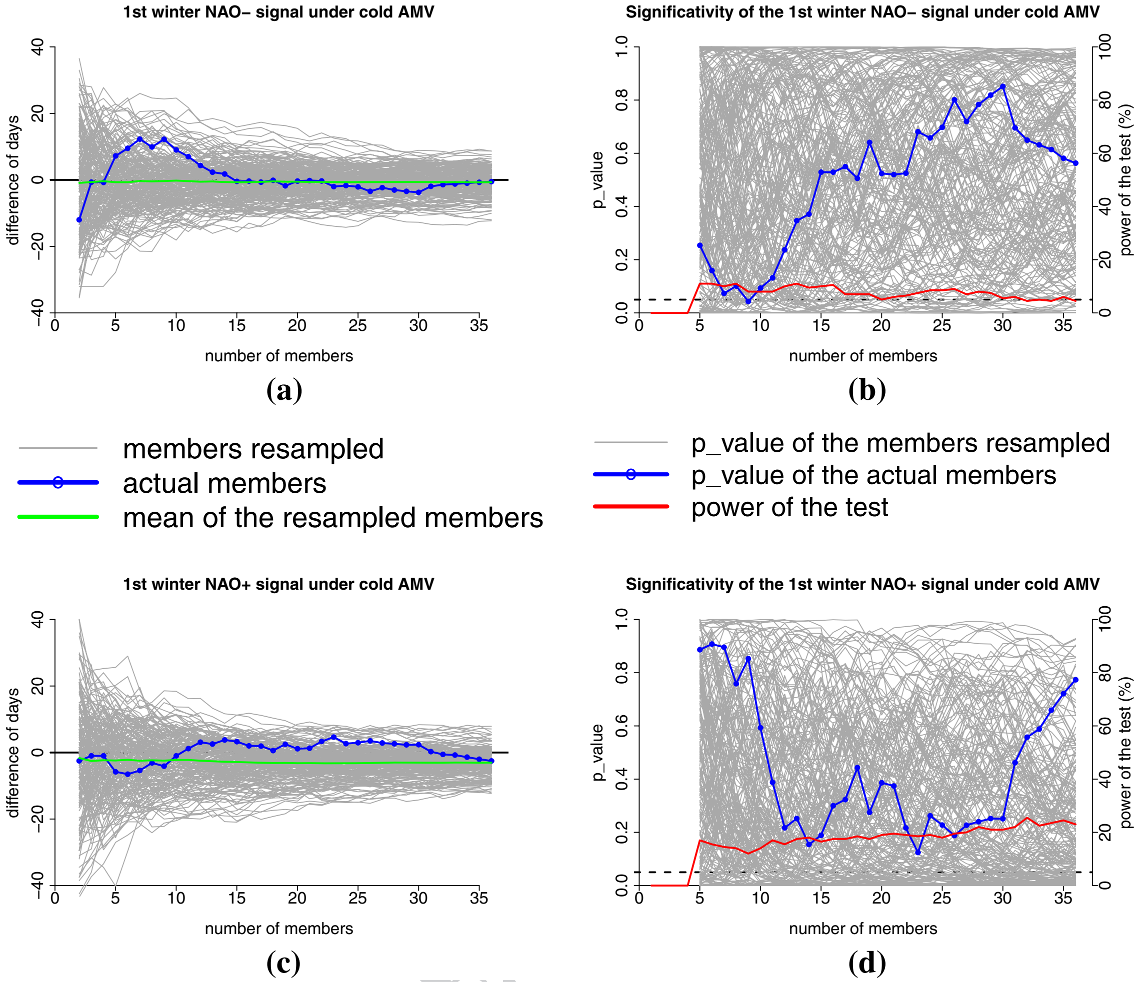

Fig. 13 Difference of NAO− (**a**) and NAO+ (**c**) WR occurrence between PinA-cold and A-cold ensemble means computed as a function of the number of members of the ensembles for the first winter. The blue curve represents the incremental actual values going from 2 to 36 members and the grey curves stand for randomly selected members among 36 based on bootstrapping (200 times with replacements). The green curve is the mean of the resampled members. Corresponding p-value for NAO− (**b**) and NAO+ (**d**) signals computed from bootstrap resampling of the difference of the WR occurrences. Computation is done from 5 to 36 members. The red curve shows the power of the test that corresponds to the percentage of tests that reach a significant WR change at the 95% confidence level (black dashed line horizontal)

size. Figure 14 thus confirms the modulation of the AMV on the volcanic-forced response of the atmospheric circulation over the North Atlantic/Europe domain. But overall, these tests objectively illustrate the very weak signal-to-noise ratio in our ensembles, which can render signals significant although they are definitely not robust if the ensembles size is not large enough.

5 Summary and discussion

A comprehensive study has been conducted using the CNRM-CM5 model to investigate the dynamical response of the climate to a Pinatubo-like eruption and its modulation by the phase of the AMV. The timing of the forced signals has been presented for the winter season and our results can be synthesized as follows.

The radiative forcing of a Pinatubo-like eruption has a strong climate signature during the first winter. A significant thermodynamical cooling is found in the tropics leading to dynamical imprints at middle-to-high latitudes through a pronounced slackening of the Hadley cell. This signal is related to a general decrease of the meridional temperature gradient leading to a global weakening of the mean westerlies circulation throughout the entire atmospheric column. Jets are equatorward shifted and the sole increase of zonal wind, albeit barely significant, is found north of 60°N, both at low level and in the stratosphere. All these responses are not conditional to the AMV phase, which solely and marginally modulates the level of decrease of the westerly

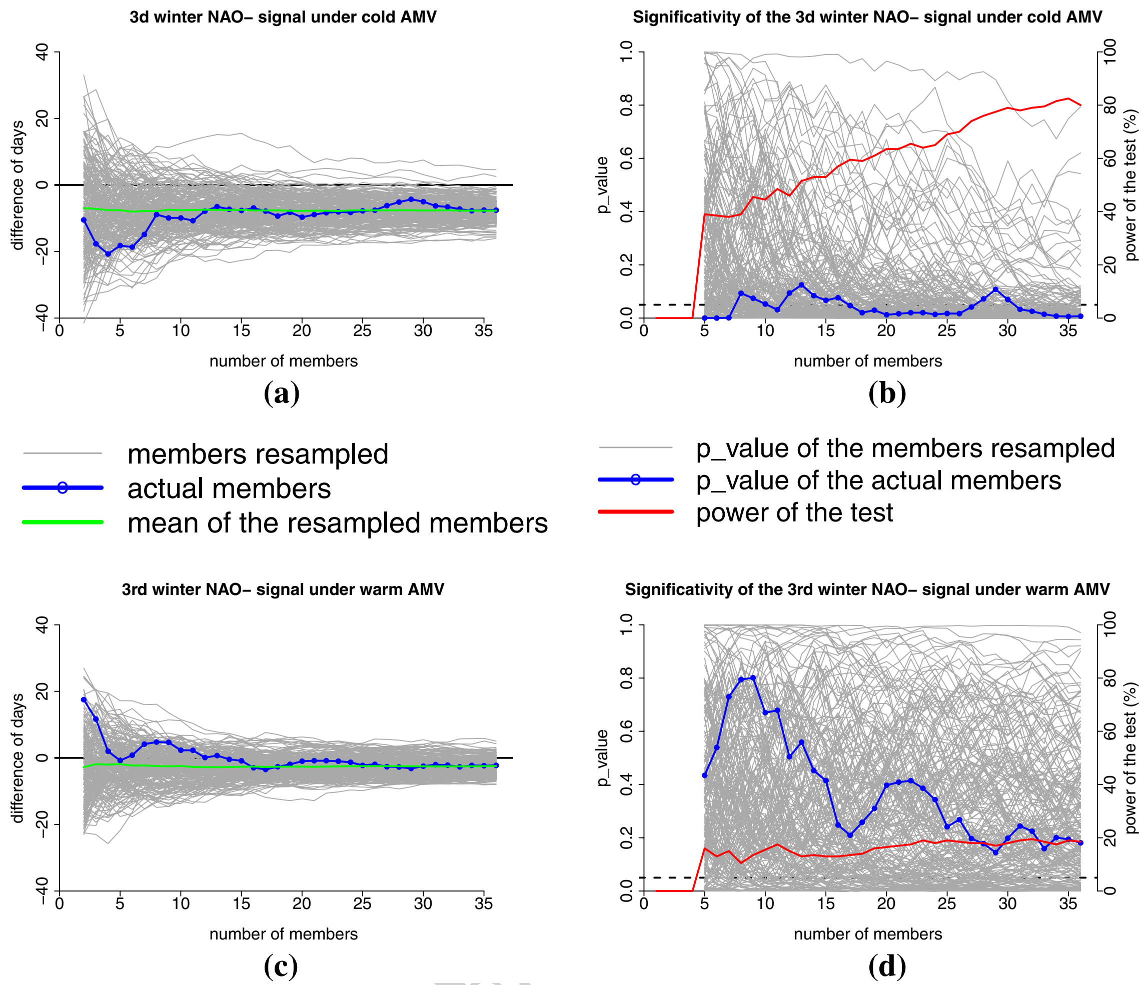

Fig. 14 Same as Fig. 9, but for the NAO− weather regime during the third winter after the eruption in cold (**a, b**) and warm (**c, d**) AMV conditions

circulation. Diagnostics based on weather regimes do not show any significant changes in the atmospheric circulation over the North Atlantic region the first winter after a volcanic eruption. This is consistent with Barnes et al. (2016) and Zambri and Robock (2016), who suggest that the volcanic imprint on the atmosphere does not project necessarily onto the natural modes of variability, even with the presence of a "winter warming" observed in Northern Europe after volcanic eruptions. It is also consistent with recent modeling studies providing consensual evidence that volcanic-forced NAO signal may not be that robust (Toohey et al. 2014; Bittner et al. 2016b). Following Zanchettin et al. (2012)'s recommendation to interpret changes within a probabilistic rather than deterministic approach, we show here that (i) a small ensemble size could lead to misleading conclusions because of very weak signal-to-noise ratio and (ii) statistical significance should be carefully evaluated. In line with Bittner et al. (2016b), we confirm that large ensembles are needed.

Over the North Atlantic, the most prominent response to a Pinatubo-eruption is found during the third winter in CNRM-CM5. Results show a decrease in the probability of occurrence of NAO− regimes, and cold AMV conditions further amplify this NAO− deficit. Such a response is not directly due to the volcanic radiative forcing that is almost gone at that time; it is related instead to the delayed influence of the ocean-sea ice system, which has integrated the volcanic-induced energy deficit at the surface. In our model, we show that the NAO− deficit is related to (i) tropical-extratropical teleconnection and (ii) feedback between Arctic SIE and North Atlantic atmospheric dynamics.

More specifically, la Niña-like conditions tend to emerge in Year 3 in response to volcanic forcing. Recent papers based on modeling approaches suggest that El Niño events are favored in Year 1 or 2. The pendular tendency for ENSO would then explain the La Niña event that we detect in Year 3 in our sensitivity experiment. Cold ENSO events have been shown in the literature to favor NAO+ circulation, which is "translated" here into NAO− deficit within the weather regime paradigm. This interpretation is particularly relevant to investigate the impact of the volcanoes over Europe since each regime is associated with specific temperature and rainfall extreme events (Slonosky and Yiou 2001). The fact that NAO− is inhibited would thus reduce the risk of cold waves to happen during the third winter after the eruption.

In addition, anomalously high SIE in autumn of Year 3 in the Arctic is hypothesized to act as an inhibitor of NAO−. This intrinsic relationship has been evidenced in our model with a 850 year experiment. The fact that La Niña conditions are stronger in AMV cold conditions and that SIE anomalies concurrently reach record-high values possibly explains the amplification of the NAO− reduction when the volcanoes erupt in cold versus warm AMV phase. The non-linearity would come from sea ice-atmosphere interaction and from diabatic heating and convection anomalies at the origin of tropical-extratropical teleconnection, which are both well known to be dependent on mean background state. Even for Year 3 where the forced-signal is the strongest in the North Atlantic, it is worth mentioning again that a minimum of 36 members is required to be fully confident on the dynamical response (p-value < 0.05 and power of test higher than 80%). This further confirms the low signal-to-noise level in the extratropical dynamics.

Limitation of our study may rely on the use of the low-top configuration of CNRM-CM5, which potentially inhibits the extratropical changes in response to volcanic eruptions. Further research is needed to investigate the volcanic-forced response of the polar vortex as well as its associated tri-dimensional teleconnections, using (i) ocean–atmosphere coupled models with well-resolved stratospheric processes but also (ii) large ensembles to correctly estimate the signal-to-noise ratio. Combining the two is still a challenge today because of limited computer resources. The use of more realistic time–space structure and spectral dependency of the volcanic forcing in models is also a pathway for progress. These issues and obstacles will be tackled within VolMIP (Zanchettin et al. 2016), a project in which the latest state-of-the-art stratospheric aerosol datasets are provided for multi-model coordinated studies.

A second limitation may rely on the experimental setup used here to assess the modulation of the Pinatubo-forced response by the AMV. We chose the extreme phases of the AMV from the piControl experiment to get two oceanic distinct initial conditions and we only perturbed the atmosphere to generate our ensembles. This setup has been inspired by Branstator and Teng (2010) who tackled issues related with initial conditions when investigating decadal predictability. At short lead-time, the AMV-forced signal might thus be perturbed by anomalies that are present in the ocean initial conditions of the ensembles outside the Atlantic, such as ENSO. Indeed, in Fig. 10, we show that A-cold ensembles have been initialized during an El Niño, whereas neutral ENSO conditions are used for A-Warm ensembles. Additionally, the Pacific Decadal Oscillation (Newman et al. 2016) is positive in A-Warm but neutral in A-cold conditions (not shown). We cannot rule out the fact that these oceanic modes may have biased the estimation of the modulation by the AMV of the volcanic-forced signal. To firmly conclude, additional experiments are needed using so-called "macro" perturbation to generate the ensembles (Hawkins et al. 2016). Such a protocol will be adopted in VolMIP (Zanchettin et al. 2016).

Finally, the AMV phases in CNRM-CM5 could be interpreted as changes in mean background climate state considering the global nature of the related anomalies (Fig. 4). If the listed limitations are not entirely prohibitive and the volcanic-forced signals are truly stronger when the North Atlantic is colder as documented here (Fig. 4a), the impact of a future Pinatubo-type eruption on the NAO could be lowered in the context of global warming and in particular due to the rapid sea ice disappearance in the Arctic. Dedicated multi-model experiments to test the sensitivity of the volcanic-forced response to the mean climate state will be required though to confirm this hypothesis.

Acknowledgements This research was carried out within the projects: (i) MORDICUS funded by the French Agence Nationale de la Recherche (ANR-13-SENV-0002-02); (ii) SPECS funded by the European Commission's Seventh Framework Research Programme under the grant agreement 308378; (iii) VOLCADEC funded by the Spanish program MINECO/FEDER (ref. CGL2015-70177-R). We thank Javier Garcia-Serrano for its comments about the NAO precursors, Omar Bellprat for its suggestions concerning the statistical analysis and François Massonnet for its recommendations in terms of graphical presentation. CC is grateful to Marie-Pierre Moine, Laure Coquart and Isabelle Dast for technical help to run the model. Computer resources have been provided by Cerfacs. We thank the two anonymous referees for their useful comments and suggestions to improve this manuscript.

References

Adams JB, Mann ME, Ammann CM (2003) Proxy evidence for an El Nino-like response to volcanic forcing. Nature 426(6964):274–278. https://doi.org/10.1038/nature02101

Ammann CM, Joos F, Schimel DS, Otto-Bliesner BL, Tomas RA (2007) Solar influence on climate during the past millennium: results from transient simulations with the NCAR climate system model. Proc Nat Acad Sci 104(10):3713–3718. https://doi.org/10.1073/pnas.0605064103

Baldwin MP, Dunkerton TJ (2001) Stratospheric harbingers of anomalous weather regimes. Science 294(5542):581–584. https://doi.org/10.1126/science.1063315

Barnes EA, Solomon S, Polvani LM (2016) Robust wind and precipitation responses to the Mount Pinatubo eruption, as simulated in the CMIP5 models. J Clim 29(13):4763–4778. https://doi.org/10.1175/JCLI-D-15-0658.1

Barrier N, Treguier AM, Cassou C, Deshayes J (2013) Impact of the winter North-Atlantic weather regimes on subtropical sea-surface height variability. Clim Dyn 41(5–6):1159–1171. https://doi.org/10.1007/s00382-012-1578-7

Bittner M, Timmreck C, Schmidt H, Toohey M, Krüger K (2016a) The impact of wave-mean flow interaction on the Northern Hemisphere polar vortex after tropical volcanic eruptions. J Geophys Res Atmos 121(10):5281–5297. https://doi.org/10.1002/2015JD024603

Bittner M, Schmidt H, Timmreck C, Sienz F (2016b) Using a large ensemble of simulations to assess the Northern Hemisphere stratospheric dynamical response to tropical volcanic eruptions and its uncertainty. Geophys Res Lett 43(17):9324–9332. https://doi.org/10.1002/2016GL070587

Bjerknes J (1966) A possible response of the atmospheric Hadley circulation to equatorial anomalies of ocean temperature. Tellus 18(4):820–829. https://doi.org/10.3402/tellusa.v18i4.9712

Bjerknes J (1969) Atmospheric teleconnections from the equatorial Pacific. Mon Weather Rev 97:163–172. https://doi.org/10.1175/1520-0493(1969)097<0163:ATFTEP>2.3.CO;2

Bony S, Stevens B, Frierson DM, Jakob C, Kageyama M, Pincus R, Shepherd TG, Sherwood SC, Siebesma AP, Sobel AH, Watanabe M (2015) Clouds, circulation and climate sensitivity. Nat Geosci 8(4):261–268. https://doi.org/10.1038/ngeo2398

Branstator G, Teng H (2010) Two limits of initial-value decadal predictability in a CGCM. J Clim 23:6292–6311. https://doi.org/10.1007/s00382-010-0977-x

Cai W, van Rensch P (2013) Austral summer teleconnections of Indo-Pacific variability: their nonlinearity and impacts on Australian climate. J Clim 26(9):2796–2810. https://doi.org/10.1175/JCLI-D-12-00458.1

Cane MA, Zebiak SE, Dolan SC (1986) Experimental forecasts of El Niño. Nature 321:827–832. https://doi.org/10.1038/321827a0

Cassou C (2008) Intraseasonal interaction between the Madden–Julian Oscillation and the North Atlantic Oscillation. Nature 455(7212):523–527. https://doi.org/10.1038/nature07286

Cassou C, Terray L, Hurrell JW, Deser C (2004) North Atlantic winter climate regimes: spatial asymmetry, stationarity with time, and oceanic forcing. J Clim 17(5):1055–1068. https://doi.org/10.1175/1520-0442(2004)017<1055:NAWCRS>2.0.CO;2

Charlton-Perez AJ et al (2013) On the lack of stratospheric dynamical variability in low-top versions of the CMIP5 models. J Geophys Res Atmos 118:2494–2505. https://doi.org/10.1002/jgrd.50125

Christiansen B (2008) Volcanic eruptions, large-scale modes in the Northern Hemisphere, and the El Niño-Southern Oscillation. J Clim 21(5):910–922. https://doi.org/10.1175/2007JCLI1657.1

Clement A, Bellomo K, Murphy LN, Cane MA, Mauritsen T, Rädel G, Stevens B (2015) The Atlantic multidecadal Oscillation without a role for ocean circulation. Science 350(6258):320–324. https://doi.org/10.1126/science.aab3980

Deser C, Sun L, Tomas RA, Screen J (2016) Does ocean-coupling matter for the northern extra-tropical response to projected Arctic sea ice loss? Geophys Res Lett 43:2149–2157. https://doi.org/10.1002/2016GL067792

Dieppois B, Durand A, Fournier M, Diedhiou A, Fontaine B, Massei N, Nouaceur Z, Sebag D (2015) Low-frequency variability and zonal contrast in Sahel rainfall and Atlantic sea surface temperature teleconnections during the last century. Theor Appl Climatol 121(1–2):139–155. https://doi.org/10.1007/s00704-014-1229-5

Dinezio PN, Deser C, Okumura Y, Karspeck A (2017) Mechanisms controlling the predictability of 2-year La Nina. Clim Dyn 1–25 https://doi.org/10.1007/s00382-017-3575-3

Ding Y, Carton JA, Chepurin GA, Stenchikov G, Robock A, Sentman LT, Krasting JP (2014) Ocean response to volcanic eruptions in Coupled Model Intercomparison Project 5 simulations. J Geophys Res Oceans 119(9):5622–5637. https://doi.org/10.1002/2013JC009780

Driscoll S, Bozzo A, Gray LJ, Robock A, Stenchikov G (2012) Coupled Model Intercomparison Project 5 (CMIP5) simulations of climate following volcanic eruptions. J Geophys Res Atmos. https://doi.org/10.1029/2012JD017607

Emile-Geay J, Seager R, Cane MA, Cook ER, Haug GH (2008) Volcanoes and ENSO over the past millennium. J Clim 21(13):3134–3148. https://doi.org/10.1175/2007JCLI1884.1

Gao LH, Yan ZW, Quan XW (2015) Observed and SST-forced multidecadal variability in global land surface air temperature. Clim Dyn 44(1–2):359–369. https://doi.org/10.1007/s00382-014-2121-9

Gastineau G, Frankignoul C (2015) Influence of the North Atlantic SST variability on the atmospheric circulation during the twentieth century. J Clim, 28(4):1396–1416. https://doi.org/10.1175/JCLI-D-14-00424.1

Graf H-F, Li Q, Giorgetta MA (2007) Volcanic effects on climate: revisiting the mechanisms. Atmos Chem Phys 7(17):4503–4511. https://doi.org/10.5194/acp-7-4503-2007

Harvey BJ, Shaffrey LC, Woollings TJ (2014) Equator-to-pole temperature differences and the extra-tropical storm track responses of the CMIP5 climate models. Clim Dyn 43(5–6):1171–1182. https://doi.org/10.1007/s00382-013-1883-9

Harvey BJ, Shaffrey LC, Woollings TJ (2015) Deconstructing the climate change response of the Northern Hemisphere wintertime storm tracks. Clim Dyn 45(9–10):2847–2860. https://doi.org/10.1007/s00382-015-2510-8

Hawkins E, Smith RS, Gregory JM, Stainforth DA (2016) Irreducible uncertainty in near-term climate projections. Clim Dyn 46(11–12):3807–3819. https://doi.org/10.1007/s00382-015-2806-8

Hirono M (1988) On the trigger of El Niño Southern Oscillation by the forcing of early El Chichón volcanic aerosols. J Geophys Res Atmos 93(D5):5365–5384. https://doi.org/10.1029/JD093iD05p05365

Hurrell JW, Kushnir Y, Ottersen G, Visbeck M (2003) An Overview of the North Atlantic Oscillation. In: Hurrell JW, Kushnir Y, Ottersen G, Visbeck M (eds) The North Atlantic Oscillation: climatic significance and environmental impact. American Geophysical Union, Washington, D.C. https://doi.org/10.1029/134GM01

Khodri M, Izumo T, Vialard J, Cassou C, Gastineau G, Lengaigne M, Mignot J, Guilyardi E, Lebas N, Ruprich-Robert Y, Robock A, McPhaden MJ (2017) How tropical explosive volcanic eruptions trigger El Niño events. Nat Commun (in press)

Knight JR, Allan RJ, Folland CK, Vellinga M, Mann ME (2005) A signature of persistent natural thermohaline circulation cycles in observed climate. Geophys Res Lett. https://doi.org/10.1029/2005GL024233

Kodera K (1994) Influence of volcanic eruptions on the troposphere through stratospheric dynamical processes in the northern hemisphere winter. J Geophys Res 99(D1):1273–1282. https://doi.org/10.1029/93JD02731

Labitzke K, McCormick MP (1992) Stratospheric temperature increases due to Pinatubo aerosols. Geophys Res Lett 19(2):207–210. https://doi.org/10.1029/91GL02940

Maher N, McGregor S, England MH, Gupta AS (2015) Effects of volcanism on tropical variability. Geophys Res Lett 42(14):6024–6033. https://doi.org/10.1002/2015GL064751

Marshall AG, Scaife AA, Ineson S (2009) Enhanced seasonal prediction of european winter warming following volcanic eruptions. J Clim 22(23):6168–6180. https://doi.org/10.1175/2009JCLI3145.1

Martin ER, Thorncroft C, Booth BBB (2014) The multidecadal Atlantic SST-sahel rainfall teleconnection in CMIP5 simulations. J Clim 27:784–806. https://doi.org/10.1175/JCLI-D-13-00242.1

McCarthy GD, Haigh ID, Hirschi JJM, Grist JP, Smeed DA (2015) Ocean impact on decadal Atlantic climate variability revealed by sea-level observations. Nature 521(7553):508–510. https://doi.org/10.1038/nature14491

Michelangeli PA, Vautard R, Legras B (1995) Weather regimes: recurrence and quasi stationarity. J Atmos Sci 52(8):1237–1256. https://doi.org/10.1175/1520-0469(1995)052<1237:WRRAQS>2.0.CO;2

Miles MW, Divine DV, Furevik T, Jansen E, Moros M, Ogilvie AE (2014) A signal of persistent Atlantic multidecadal variability in Arctic sea ice. Geophys Res Lett 41(2):463–469. https://doi.org/10.1002/2013GL058084

Mudelsee M (2014) Climate time series analysis, atmospheric and oceanographic sciences library, Eds. Springer International Publishing, New York, p. 454, https://doi.org/10.1007/978-3-319-04450-7

Newman M, Alexander MA, Ault TR, Cobb KM, Deser C, Di Lorenzo E, Mantua NJ, Miller AJ, Minobe S, Nakamura H, Schneider N (2016) The Pacific decadal Oscillation, revisited. J Clim 29(12):4399–4427. https://doi.org/10.1175/JCLI-D-15-0508.1

Ohba M, Shiogama H, Yokohata T, Watanabe M (2013) Impact of strong tropical volcanic eruptions on ENSO simulated in a coupled GCM. J Clim 26(14):5169–5182. https://doi.org/10.1175/JCLI-D-12-00471.1

Omrani N-E, Keenlyside NS, Bader J, Manzini E (2014) Stratosphere key for wintertime atmospheric response to warm atlantic decadal conditions. Clim Dyn 42:3–4. https://doi.org/10.1007/s00382-013-1860-3 649–663

Ortega P, Lehner F, Swingedouw D, Masson-Delmotte V, Raible CC, Casado M, Yiou P (2015) A model-tested North Atlantic Oscillation reconstruction for the past millennium. Nature 523(7558):71–74. https://doi.org/10.1038/nature14518

Ottera OH, Bentsen M, Drange H, Suo L (2010) External forcing as a metronome for Atlantic multidecadal variability. Nat Geosci 3(10):688. https://doi.org/10.1038/NGEO995

Oudar T, Sanchez-Gomez E, Chauvin F, Cattiaux J, Terray L, Cassou C (2017) Respective roles of direct GHG radiative forcing and induced Arctic sea ice loss on the Northern Hemisphere atmospheric circulation. Clim Dyn. https://doi.org/10.1007/s00382-017-3541-0

Pausata FS, Karamperidou C, Caballero R, Battisti DS (2016) ENSO response to high-latitude volcanic eruptions in the Northern Hemisphere: the role of the initial conditions. Geophys Res Lett 43(16):8694–8702. https://doi.org/10.1002/2016GL069575

Peings Y, Magnusdottir G (2014) Response of the wintertime Northern Hemisphere atmospheric circulation to current and projected Arctic sea ice decline: a numerical study with CAM5. J Clim 27(1):244–264. https://doi.org/10.1175/JCLI-D-13-00272.1

Robock A (2000) Volcanic eruptions and climate. Rev Geophys 38(2):191–219. https://doi.org/10.1029/1998RG000054

Robock A, Mao J (1995) The volcanic signal in surface temperature observations. J Clim 8(5):1086–1103. https://doi.org/10.1175/1520-0442(1995)008<1086:TVSIST>2.0.CO;2

Robson J, Ortega P, Sutton R (2016) A reversal of climatic trends in the North Atlantic since 2005. Nat Geosci 9:513–517. https://doi.org/10.1038/ngeo2727

Ruprich-Robert Y, Cassou C (2015) Combined influences of seasonal East Atlantic Pattern and North Atlantic Oscillation to excite Atlantic multidecadal variability in a climate model. Clim Dyn 44:229–253. https://doi.org/10.1007/s00382-014-2176-7

Ruprich-Robert Y, Msadek R, Castruccio F, Yeager S, Delworth T, Danabasoglu G (2017) Assessing the climate impacts of the observed Atlantic multidecadal variability using the GFDL CM2.1 and NCAR CESM1 global coupled models. J Clim 30(8):2785–2810. https://doi.org/10.1175/JCLI-D-16-0127.1

Scaife AA, Knight JR, Vallis GK, Folland CK (2005) A stratospheric influence on the winter NAO and North Atlantic surface climate. Geophys Res Lett 32:L18715. https://doi.org/10.1029/2005GL023226

Shindell DT, Schmidt GA, Mann ME, Faluvegi G (2004) Dynamic winter climate response to large tropical volcanic eruptions since 1600. J Geophys Res 109(D5):D05104. https://doi.org/10.1029/2003JD004151

Siegert S, Bellprat O, Ménégoz M, Stephenson DB, Doblas-Reyes FJ (2017) Detecting improvements in forecast correlation skill: statistical testing and power analysis. Mon Weather Rev 145(2):437–450. https://doi.org/10.1175/MWR-D-16-0037.1

Slonosky VC, Yiou P (2001) The North Atlantic Oscillation and its relationship with near surface temperature. Geophys Res Lett 28:807–810. https://doi.org/10.1029/2000GL012063

Stenchikov G, Robock A, Ramaswamy V, Schwarzkopf MD, Hamilton K, Ramachandran S (2002) Arctic Oscillation response to the 1991 Mount Pinatubo eruption: effects of volcanic aerosols and ozone depletion. J Geophys Res Atmos 107(D24):4803. https://doi.org/10.1029/2002JD002090

Stenchikov G, Hamilton K, Robock A, Ramaswamy V, Schwarzkopf MD (2004) Arctic Oscillation response to the 1991 Pinatubo eruption in the SKYHI general circulation model with a realistic quasi-biennial Oscillation. J Geophys Res 109(D3):D03112. https://doi.org/10.1029/2003JD003699

Stenchikov G, Hamilton K, Stouffer RJ, Robock A, Ramaswamy V, Santer B, Graf HF (2006) Arctic Oscillation response to volcanic eruptions in the IPCC AR4 climate models. J Geophys Res Atmos D07107. https://doi.org/10.1029/2005JD006286

Stenchikov G, Delworth TL, Ramaswamy V, Stouffer RJ, Wittenberg A, Zeng F (2009) Volcanic signals in oceans. J Geophys Res 114:D16104. https://doi.org/10.1029/2008JD011673

Sun C, Li J, Jin FF (2015a) A delayed Oscillator model for the quasi-periodic multidecadal variability of the NAO. Clim Dyn 45(7–8):2083–2099. https://doi.org/10.1007/s00382-014-2459-z

Sun L, Deser C, Tomas RA (2015b) Mechanisms of Stratospheric and Tropospheric Circulation Response to Projected Arctic Sea Ice Loss. J Clim 28(19):7824–7845. https://doi.org/10.1175/JCLI-D-15-0169.1

Sutton RT, Dong B (2012) Atlantic Ocean influence on a shift in European climate in the 1990s. Nat Geosci 5(11):788–792. https://doi.org/10.1038/ngeo1595

Swingedouw D, Ortega P, Mignot J, Guilyardi E, Masson-Delmotte V, Butler PG et al (2015) Bidecadal North Atlantic ocean circulation variability controlled by timing of volcanic eruptions. Nat commun 6:6545. https://doi.org/10.1038/ncomms7545

Swingedouw D, Mignot J, Ortega P, Khodri M, Ménégoz M, Cassou C, Hanquiez V (2017) Impact of explosive volcanic eruptions on the main climate variability modes. Global Planet Change 150:24–45. https://doi.org/10.1016/j.gloplacha.2017.01.006

Tanaka HL, Tokinaga H (2002) Baroclinic instability in high latitudes induced by polar vortex: a connection to the Arctic Oscillation. J Atmos Sci 59(1):69–82. https://doi.org/10.1175/1520-0469(2002)059<0069:BIIHLI>2.0.CO;2

Taylor KE, Stouffer RJ, Meehl GA (2012) An overview of CMIP5 and the experiment design. Bull Am Meteorol Soc 93(4):485. https://doi.org/10.1175/BAMS-D-11-00094.1

Terray L, Cassou C (2002) Tropical Atlantic sea surface temperature forcing of quasi-decadal climate variability over the North Atlantic-European region. J Clim 15(22):3170–3187. https://doi.org/10.1175/1520-0442(2002)015<3170:TASSTF>2.0.CO;2

Thomas MA, Giorgetta MA, Timmreck C, Graf H-F, Stenchikov G (2009) Simulation of the climate impact of Mt. Pinatubo eruption using ECHAM5 - Part 2: Sensitivity to the phase of the QBO and ENSO. Atmos Chem Phys 9(9):3001–3009. https://doi.org/10.5194/acp-9-3001-2009

Toohey M, Krüger K, Bittner M, Timmreck C, Schmidt H (2014) The impact of volcanic aerosol on the Northern Hemisphere stratospheric polar vortex: mechanisms and sensitivity to forcing structure. Atmos Chem Phys 14(23):13063–13079. https://doi.org/10.5194/acp-14-13063-2014

Trenberth KE, Branstator GW, Karoly D, Kumar A, Lau N-C, Ropelewski C (1998) Progress during TOGA in understanding and modeling global teleconnections associated with tropical sea surface temperatures. J Geophys Res 103(324):14291–14214. https://doi.org/10.1029/97JC01444

Ullmann A, Fontaine B, Roucou P (2014) Euro-Atlantic weather regimes and Mediterranean rainfall patterns: present-day variability and expected changes under CMIP5 projections. Int J Climatol 34(8):2634–2650. https://doi.org/10.1002/joc.3864

Vautard R (1990) Multiple weather regimes over the North Atlantic: analysis of precursors and successors. Mon Weather Rev 118(10):2056–2081. https://doi.org/10.1175/1520-0493(1990)118<2056:MWROTN>2.0.CO;2

Voldoire A, Sanchez-Gomez E, y Mélia DS, Decharme B, Cassou C, Sénési S et al (2013) The CNRM-CM5. 1 global climate model: description and basic evaluation. Clim Dyn 40(9–10):2091–2121. https://doi.org/10.1007/s00382-011-1259-y

Zambri B, Robock A (2016), Winter warming and summer monsoon reduction after volcanic eruptions in Coupled Model Intercomparison Project 5 (CMIP5) simulations. Geophys Res Lett 43(20):10920–10928. https://doi.org/10.1002/2016GL070460

Zanchettin D, Timmreck C, Graf H-F, Rubino A, Lorenz S, Lohmann K, Krueger K, Jungclaus JH (2012) Bi-decadal variability excited in the coupled ocean-atmosphere system by strong tropical volcanic eruptions. Clim Dyn 39:419–444. https://doi.org/10.1007/s00382-011-1167-1

Zanchettin D, Timmreck C, Bothe O, Lorenz SJ, Hegerl G, Graf HF et al (2013a) Delayed winter warming: a robust decadal response to strong tropical volcanic eruptions? Geophys Res Lett 40(1):204–209. https://doi.org/10.1029/2012GL054403

Zanchettin D, Bothe O, Graf HF, Lorenz SJ, Luterbacher J, Timmreck C, Jungclaus JH (2013b) Background conditions influence the decadal climate response to strong volcanic eruptions. J Geophys Res Atmos 118(10):4090–4106. https://doi.org/10.1002/jgrd.50229

Zanchettin D, Khodri M, Timmreck C, Toohey M, Schmidt A, Gerber EP et al (2016) The Model Intercomparison Project on the climatic response to Volcanic forcing (VolMIP): experimental design and forcing input data for CMIP6. Geosci Model Dev 9(8):2701–2719. https://doi.org/10.5194/gmd-9-2701-2016

Journal : Large 382	Article No : 3986	Pages : 21	MS Code : CLDY-D-16-00926	Dispatch : 30-10-2017

Journal:	**382**
Article:	**3986**

Springer
the language of science

Author Query Form

Please ensure you fill out your response to the queries raised below and return this form along with your corrections

Dear Author

During the process of typesetting your article, the following queries have arisen. Please check your typeset proof carefully against the queries listed below and mark the necessary changes either directly on the proof/online grid or in the 'Author's response' area provided below

Query	Details Required	Author's Response
AQ1	Author: The citation Christiansen et al. 2008 has been changed to Christiansen 2008. Please check here and in subsequent occurrences, and correct if necessary.	
AQ2	Author: The citation Gastineau et al. 2015 has been changed to Gastineau and Frankignoul 2015. Please check here and in subsequent occurrences, and correct if necessary.	
AQ3	Author: Reference: References Robock et al. 1995, Vautard 1990, Cane and Zebiak 1985 were mentioned in the manuscript; however, this were not included in the reference list. As a rule, all mentioned references should be present in the reference list. Please provide the reference details to be inserted in the reference list.	
AQ4	Author: The citation Bjerknes et al. (1966, 1969) has been changed to Bjerknes (1966, 1969). Please check here and in subsequent occurrences, and correct if necessary.	
AQ5	Author: The citation Cai et al. 2013 has been changed to Cai and Rensch 2013. Please check here and in subsequent occurrences, and correct if necessary.	
AQ6	Author: Reference: References Clement et al. 2015, Kodera 1994, Miles et al. 2014, Robson et al. 2016, Ullmann et al. 2014 were provided in the reference list; however, this were not mentioned or cited in the manuscript. As a rule, if a citation is present in the text, then it should be present in the list. Please provide the location of where to insert the reference citation in the main body text.	
AQ7	Author: Please update Ref. Khodri et al. (2017) with complete details, if possible.	
AQ8	Author: Please check and confirm the location of the publisher for Ref Mudelsee (2014).	
AQ9	Author: Please check and confirm the year of publication for Ref Thomas et al. 2009.	